TRAUMATIC BRAIN INJURY (TBI) PREDICTION IN PEDESTRIAN COLLISIONS

A Thesis
Presented in Partial Fulfillment for the Requirements for
the Degree Master of Science in the
Graduate School of The Ohio State University

By
Kyle A. Ott, B.S.M.E.

* * * * *

The Ohio State University

2005

Master's Examination Committee:
Dr. Dennis A Guenther, Adviser
Dr. John F Wiechel, Co-Adviser

Approved by

Dennis A. Guenther

Adviser

Department of
Mechanical Engineering

Copyright by

Kyle A. Ott

2005

ABSTRACT

Pedestrians account for roughly 12% of all motor vehicle related fatalities in the United States, which equates to approximately 4,700 deaths per year. Head injuries are the most common cause of death in these accidents. Current test procedures around the world involve launching a projectile headform into vehicle structures to assess aggressiveness toward pedestrians. The Head Injury Criterion (HIC) uses linear accelerations from a pedestrian headform to assess impact severity, which is in turn dictated by the head impact velocity and vehicle stiffness. Vehicle exterior contours or underhood structures often impart a rotational component to the headform upon impact as well as affecting the wrap around distance (WAD). In the past several years, evidence has indicated that these types of rotational accelerations influence injury. The objective of this study was to examine the relationships between vehicle characteristics and head injury using a combination of computer modeling, experimental testing, and accident data. Analytical tools could then be constructed based on these quantified relationships to facilitate pedestrian-safe vehicle design.

A multi-body, finite element-based headform model has previously been developed to exhibit response characteristics consistent with the International Harmonization Research Activities (IHRA) adult and child pedestrian headforms. In the

current study, a series of simulations with this model was conducted using a wide range of impact velocities and stiffness values, producing a distribution of HIC values. Experimental test data was used to determine where a sample of the U.S. fleet falls in the simulated HIC matrix. The second phase of this research involved the investigation of head injury mechanisms through case reconstruction. Full-scale pedestrian case reconstructions were done in MADYMO to acquire linear and angular accelerations of the pedestrian's head. These accelerations were then entered into the Simulated Injury Monitor (SIMon) algorithm to predict brain injury based on both translational and rotational acceleration. These predicted injuries were then compared to those documented in the case. The third phase of this study involved the relation of certain accident geometric parameters to injury using statistical software to analyze the Pedestrian Crash Data Study (PCDS) data and derive relations. This would help lead to an equation that would predict probability of brain injury based on certain geometric characteristics.

Three different tools were developed from this study. The first tool is a HIC predictive algorithm that gave HIC as a function of head impact velocity and linear stiffness. The second tool is a reconstruction process through which both traumatic brain injury and skull fracture may be predicted. The third tool is a relation between WAD as a function of vehicle impact speed and top transition point normalized by pedestrian height as well as a set of probability curves of injury as a function of vehicle speed.

Dedicated to

My family, both old and new

ACKNOWLEDGMENTS

I would like to thank my advisers, Dr. Dennis Guenther and Dr. John Wiechel for all of their advice and direction through this project, as well as their help in correcting the many typographical and grammatical errors I have. I would like to thank Jason Stammen for continually brainstorming new ideas with me and being so patient for every meeting. Ann Mallory for all of her help with the statistical analysis involved as well as her help in balancing both Jason and I. I would like to thank David Hyder for his help in guiding me through the experimental testing of the project as well as helping me always acquire the needed equipment for our testing. I would like to thank my parents for their advice, love and sharing of their own experiences in graduate school. I would like to thank my lovely fiancé for always supporting me and being so patient with me as well as her family for continually feeding me. And finally I would like to thank God for listening to all my prayers and delivering on so much.

VITA

December, 28 1981 .... Born - Nyon, Switzerland

2004... B.S.M.E., The Ohio State University.

2004 – 2005... Graduate Research Assistant,
The Ohio State University

FIELDS OF STUDY

Major Field: Mechanical Engineering, Biomechanics

TABLE OF CONTENTS

LIST OF TABLES

LIST OF FIGURES

Figure **Page**

LIST OF SYMBOLS

$a(t)$: the resultant linear acceleration time history

g: acceleration of gravity (9.81 m/s^2)

h: drop height

KE: Kinetic energy of the headform immediately before impact

m: mass of the headform

t_i: time point for a certain time interval

θ: Given impact angle

V_{90} : Corresponding 90° impact velocity

V_θ : Given impact velocity

v: impact velocity of the headform

V_S : Velocity applied to the headform in MADYMO

LIST OF ABBREVIATIONS

AIS – Abbreviated Injury Scale

ASDH- Acute Subdural Hematoma

BH – Bumper Height

CSF – Cerebral Spinal Fluid

CSDM – Cumulative Strain Damage Measure

DAI- Diffuse Axonal Injury

DDM – Dilation Damage Measure

FE – Finite Element

GTR – Global Technical Regulation

HIC – Head Injury Criterion

HL – Hood Length

HLE – Hood Leading Edge

MADYMO - Mathematical Dynamic Model

NHTSA – National Highway Traffic Safety Administration

PCDS – Pedestrian Crash Data Study

PH – Pedestrian Height

RMDM – Relative Motion Damage Measure

SIMon – Simulated Injury Monitor

TBI – Traumatic Brain Injury

VS – Vehicle Speed

WAD – Wrap Around Distance

CHAPTER 1

INTRODUCTION

Head injuries continue to be one of the most frequent consequences of automobile accidents. Recent studies show approximately fifty-percent of all severe skull-brain trauma results from automotive accidents [7]. Pedestrian fatalities in the United States account for more than 10% of all traffic related fatalities with the percentages being larger in many countries of the world. The majority of these deaths result from a head injury. These traumatic brain injuries (TBI) have far reaching emotional, social and economic implications to society. Since treatment of these brain injuries and rehabilitation techniques are limited, an effective alternative is the prevention and mitigation of these injuries [7]. This effort to reduce pedestrian head injury mechanisms must be understood in order to evaluate the effectiveness of vehicle countermeasures using applicable injury criteria.

The most commonly used criterion for determining the likelihood of head injury is the Head Injury Criterion (HIC). HIC is derived from the resultant acceleration measured at the center of gravity of a headform. This criterion was developed from a comparison of the Wayne State Tolerance Curve (WSTC) and Gadd Severity Index (GSI) [19] and is defined by the following equation:

$$\mathrm{HIC} = \max_{t_1, t_2 \to} \left\{ (t_2 - t_1) \left[\frac{1}{(t_2 - t_1)} \int_{t_1}^{t_2} a(t)dt \right]^{2.5} \right\} \quad (1)$$

Where: *a(t)* = the resultant linear acceleration time history

t_1 and t_2 = two points during the total time interval that would maximize the HIC value

(t_2-t_1) = time interval over which HIC is calculated [19]

To determine HIC, a time interval is first set. Commonly used time intervals are 15 and 36 ms. Since this time interval has a large effect on the HIC calculation, determination of a proper time interval is important. Although HIC is somewhat limited in that it only considers linear accelerations, it has been shown to be a good indicator for skull fracture and has been used almost universally in crash injury research and prevention since its introduction [6]. However, there have also been several studies that indicate TBI is not only a function of linear acceleration but also rotational acceleration and the resulting strain within the brain itself. This evidence has created a need for other criteria in the prediction of brain injury [5, 17, 19, 20].

Previous work using simulation software has been completed to help increase understanding and simulation of brain injury. The Wayne State University brain injury model (WSUBIM) can simulate diffuse axonal injuries as well as the brain's directional sensitivity to impacts, the resulting intracranial pressure, and maximum shear stress [23].

The original model of the human skull and brain was later updated to also include facial structures. The WSUBIM model was also updated in order to simulate both direct and indirect impacts over a wide range of impact severities. The model itself consists of a finite element mesh containing over 280,000 nodes and 314,500 elements developed in HyperMesh® and executed using the explicit finite element solver PAM-CRASH™. This model was then validated using published cadaveric test data [2, 5, 11, 13, 18]. However, due to the incredibly detailed finite element (FE) mesh, one simulation with a length of 50 ms required 60 hours on an IBM SP supercomputer with 5 parallel CPUs making this model very cumbersome in terms of run time and hardware required.

Another far less complicated model was developed by Kamalakkanaan to simulate the current International Harmonization Research Activities (IHRA) pedestrian headform [8]. This model consists of a finite element hemisphere (963 nodes and 600 elements) to represent the vinyl skin that covers half of a multi-body sphere, which represents the aluminum core and accelerometer mount. Validation of the model was performed by comparing laboratory and simulated certification drop test acceleration profiles and HIC values. The simulations were executed in MADYMO (Mathematical Dynamic Model), a program that simulates the dynamic behavior of physical systems, emphasizing the analysis of vehicle collisions and assessing injuries sustained (MADYMO theory manual [17]). Once validation was complete, a parameter analysis was conducted to examine the sensitivity of the model's response to IHRA specified geometric constraints [8].

An injury-based model developed by Takhounts was validated with both human and baboon experimental brain data [17]. SIMon (Simulated Injury Monitor) is designed to efficiently simulate an impact up to 150 ms in duration. This model consists of a finite element model of the skull and brain that includes several different structures of the brain including the skull, Dura-Cerebral Spinal Fluid (CSF) layer, brain, Falx Cerebri and bridging veins. It was originally intended to model the Hybrid III 50th percentile male head with a mass of 4.7 kg but has since been adapted to other dummy sizes. In all, the model contains 10475 nodes and 7852 elements and has demonstrated the ability to predict the likelihood of several different injuries including diffuse axonal injuries (DAI), brain contusions and acute subdural hematomas. To determine the likelihood of each of these injuries, SIMon uses several different correlates to injury. Cumulative strain damage measure (CSDM) is a correlate for DAI based on the finding that this injury is associated with the cumulative volume of brain tissue experiencing tensile strains over a predefined critical level found from animal experiments [1, 9, 12, 14]. Dilation damage measure (DDM) is a correlate for contusions and involves localized regions where stress in the brain result in negative pressures that exceed values required to produce contusions, leading to tissue damage. The pressure threshold is set at 100 kPa (–14.7 psi) which corresponds to the vapor pressure of water, again established from animal impact tests [12, 14]. The spatial distribution of the volume reaching this negative pressure limit determines the likelihood of contusions. Finally, relative motion damage measure (RMDM) is a correlate for acute subdural hematoma (ASDH) injuries. This correlate predicts the potential for failure of a bridging vein at any time, *t,* by calculating the ratio of a vein's current strain to its failure strain. SIMon is able to predict these three injuries by taking linear acceleration data from the dummy head in a crash test and deriving the corresponding rotational components that have been shown to correlate with brain injury.

To help in the understanding of how to mitigate head injury in pedestrian crashes, the crash conditions leading to these types of injuries were researched. The most well known source of detailed pedestrian injury data in the United States is the Pedestrian Crash Data Study (PCDS) conducted from 1994 to 1998 [4]. The study collected detailed crash information from 550 pedestrian accidents in six major U.S. cities. This database provides all of the necessary vehicle and crash parameters required to reconstruct accident cases using computer simulation. One of the major conclusions from this study was that vehicle type and front-end profile strongly influence risk of severe injury and death to the pedestrian. Data relating vehicle characteristics to head injury mechanisms will prove critical in driving vehicle designs toward improved pedestrian safety.

The objective of this study is to link pedestrian crash characteristics such as vehicle geometry and pedestrian size to head injury risk. Such a link can be used to develop vehicle design guidelines or tools, as well as more robust injury criteria to prevent or mitigate pedestrian head injuries in the field. A vehicle-specific approach that predicts (1) where a given pedestrian's head will likely impact the vehicle, (2) what types of head injuries will likely result after contact, and (3) how to decrease the impact severity at that location would be very useful in facilitating pedestrian-friendly vehicle design. To quantify these relationships comprehensively, head component and full-body pedestrian computer models, experimental testing, and the Pedestrian Crash Data Study (PCDS) were utilized. In this study, three tools were developed to aide in this design approach. These tools are (1) a HIC predictive algorithm (HPA) formed from varying impact velocity and the stiffness of the surface impacted, (2) a reconstruction process that involves both MADYMO and SIMon to predict and analyze injuries caused by rotational acceleration, and (3) an algorithm that predicts wrap around distance (WAD), or, more specifically, the location of head contact on a vehicle front, given known vehicle and pedestrian characteristics. Finally, the HPA and reconstructions were used to assess the effectiveness of a test procedure designed to mitigate head injury (both skull and brain injury).

CHAPTER 2

METHODS

2.1 HIC Predictive Algorithm Construction

The first phase of this research focuses primarily on skull fracture and how it corresponds to various crash parameters. The HIC algorithm developed herein is an attempt to relate three different parameters, specifically HIC, velocity and stiffness. Using these parameters, a mathematical formula was developed to calculate the value of any of the three parameters as function of the other two.

For this part of the study, the IHRA headform model developed by Kamalakkanaan [8] in MADYMO was used to create a matrix of HIC values that varied both with impact velocity and stiffness of the impacted surface (Figure 1). This model had been originally validated using drop tests of the physical IHRA headform onto a rigid steel plate from different heights. For the current study, the model was validated with impacts into surfaces of varying stiffness in order to better assess the model's performance in a vehicle impact environment. The model's response needs to be consistent with the headform's response in this environment to develop a mathematical relationship between HIC and stiffness and impact velocity values. Knowledge of the front-end geometries, combined with other parameters such as impact velocity and pedestrian height, could be related through an equation to produce the corresponding head impact velocities. Using the resulting data, different front-end geometric and stiffness options could be explored in an attempt to minimize the chance of pedestrian skull fracture and brain injury for a variety of impact speeds.

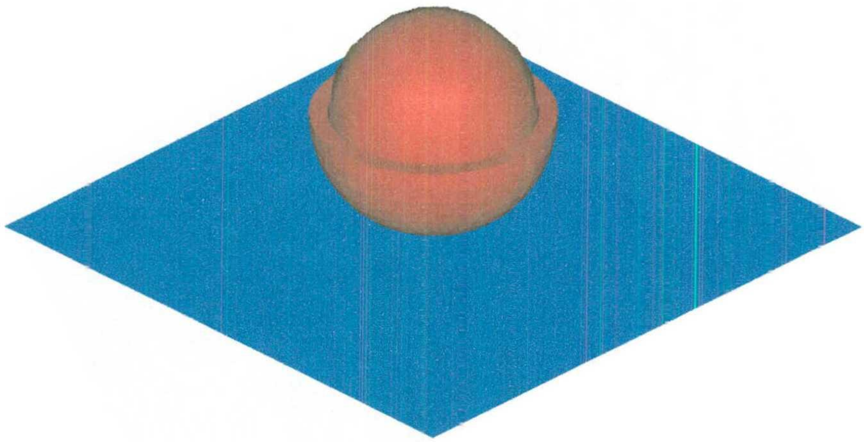

Figure 1: IHRA Headform Model [8]

To validate the model for varying values of stiffness, vehicle stiffness values were derived from an IHRA survey of experimental testing [10]. This study gave the two bounding extremes of stiffness values for car hoods (Figure 2).

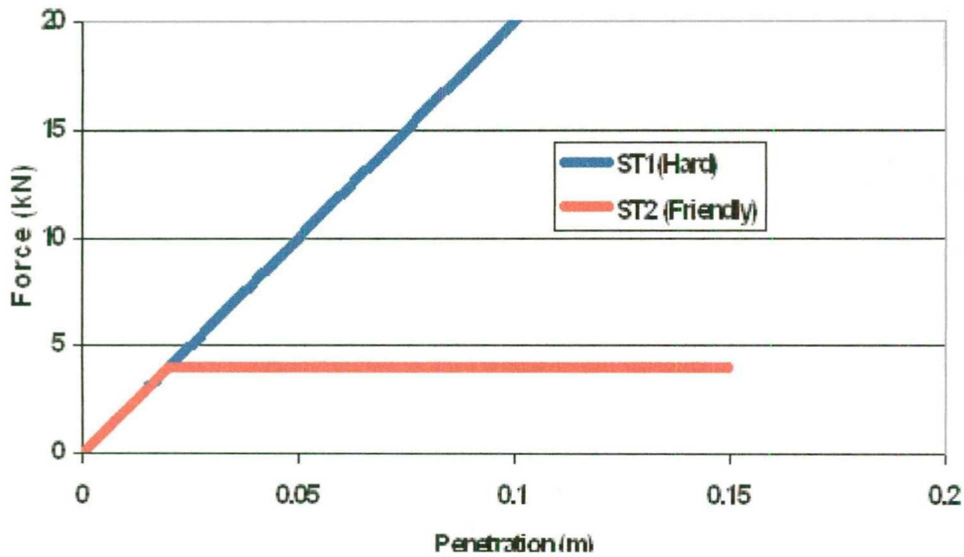

Figure 2: Vehicle stiffness curves [10]

The first series of validation tests for this model involved dropping an IHRA adult headform from a known height onto a steel plate with a spring of known stiffness attached underneath the plate to resist downward motion. Equations (2) and (3) were used to determine the velocity of the headform in MADYMO.

$$m_1 V_1 + m_2 V_2 = (m_1 + m_2) V_3 \tag{2}$$

$$V_2 = \sqrt{2gh} \tag{3}$$

m_1 = mass of the plate

V_1 = initial velocity of the plate (zero in this simulation)

m_2 = mass of the headform

V_2 = initial velocity of the headform

V_3 = velocity of the headform at impact with the plate

g = acceleration of gravity (9.81 m/s^2)

h = drop height

This approach incorporated the interaction of the two bodies (steel plate and headform) into the velocity as well as the initial velocity that was determined by the drop height. For the duration of the impact that was most critical (the deceleration of the headform and compression of the spring) it was assumed that the headform and the steel plate would experience an inelastic collision. This assumption is reflected in equation (2) and is derived from the conservation of momentum. This is not exactly the case because the steel plate and the headform did not attach to one another after impact and there was some compression of the headform skin which would act to absorb some energy and slow the headform down. However, the properties of the rubber of the headform and therefore the relative compression of the headform skin were already accounted for in the simulation and therefore assumption of conservation of momentum was a reasonable simplification of the impact. Three different springs with known stiffness properties and negligible mass were used to support the impact plate and the headform was dropped from three different heights as shown in Figure 3 and Table 1.

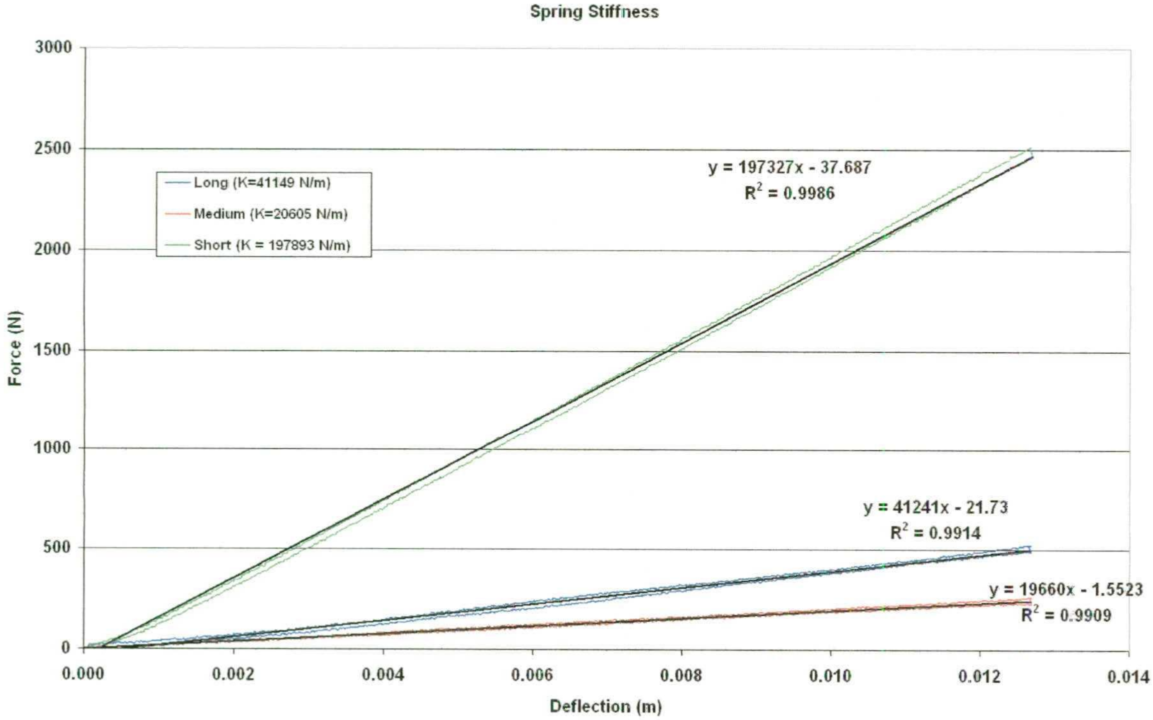

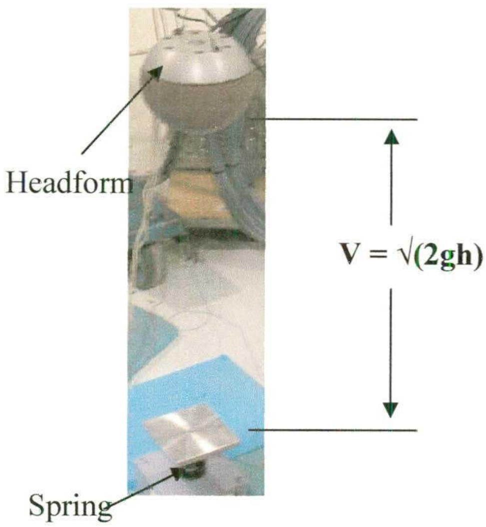

Figure 3: Spring stiffness values (top), Test setup for response validation drops (bottom)

		Calculated Impact Velocity		
		3.46 m/s	4.23 m/s	4.89 m/s
Spring Stiffness	197 kN/m	Test 1	Test 2	Test 3
	20.6 kN/m	Test 4	Test 5	Test 6
	41 kN/m	Test 7	Test 8	Test 9

Table 1: Validation Test Matrix

To validate the model at a higher velocity and at different stiffness values, a series of headform impact tests were performed on several common car hoods from the US fleet (2001 Honda Civic, 2004 GMC Savana, 2001 Ford Escape, 2003 Dodge Ram, 2004 Toyota Camry, 2004 Toyota Sienna, and 1994 Honda Civic). Several impact points on each vehicle were tested to be consistent with the proposed Global Technical Regulation (GTR) [24] and are intended to give a range of stiffness points on a vehicle. An example of one of these test setups is given in Figure 3. These tests gave a sample of real-world HIC values and provided validation of the HIC/velocity/stiffness database at a higher speed. Using the acceleration traces from these impact tests at a nominal velocity of 8.9 m/s, the applicable headform mass (4.5 kg for the adult headform, 3.5 kg for the child headform), and deflection from double-integrated acceleration, the corresponding stiffness curves of the different impact points were calculated. These tests were done at various impact angles, also consistent with the proposed GTR. However, since the headform model was validated using only vertical (perpendicular - 90^{o} impact orientation) drops, for each of these tests the corresponding 90^{o} impact velocities were calculated using the given impact angles and impact velocity using equation (4).

$$V_{90} = V_{\theta}\sin(\theta) \qquad (4)$$

V_{90} = Corresponding 90° impact velocity

V_{θ} = Given impact velocity

θ = Given impact angle

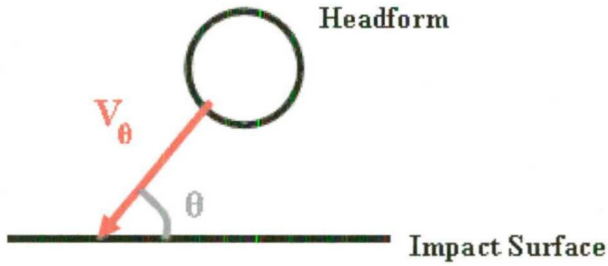

Figure 4: Impact velocity and angle diagram

This approach was verified when it was found during the course of experimentation and simulation that angled/resultant velocity (V_{θ}) and perpendicular/component velocity (V_{90}) simulated impacts gave similar HIC values for impacts with equal perpendicular velocities. Once the model was validated over the applicable range of stiffness and head impact velocities, an extensive number of iterative simulations (11 velocities x 36 stiffness values = 396) were conducted to create a database relating HIC to impact velocity and stiffness. The stiffness characteristic of the simulated impact plate varied between the two bounding extremes (shown in Figure 2) in increments of 5 kN/m. Using head-to-vehicle impact speed ratios presented by Mizuno, a head impact velocity range was also derived from vehicle impact speeds in available accident data [4]. Head impact velocity was varied from 3 m/s to 13 m/s in increments of 1 m/s.

With the headform model validated the resulting HIC values from the 396 simulations were fit using a multiple regression method in Matlab. A full quadratic fit was chosen based on the confidence bands and best fit. The Matlab output for a full quadratic fit is shown in equation (5):

$$Y = b_0 + b_1x_1 + b_2x_2 + b_3x_1x_2 + b_4{x_1}^2 + b_5{x_2}^2 \qquad (5)$$

Y = Dependent variable

x_n= Independent variable

b_n = Fit coefficients/parameter estimates given by Matlab

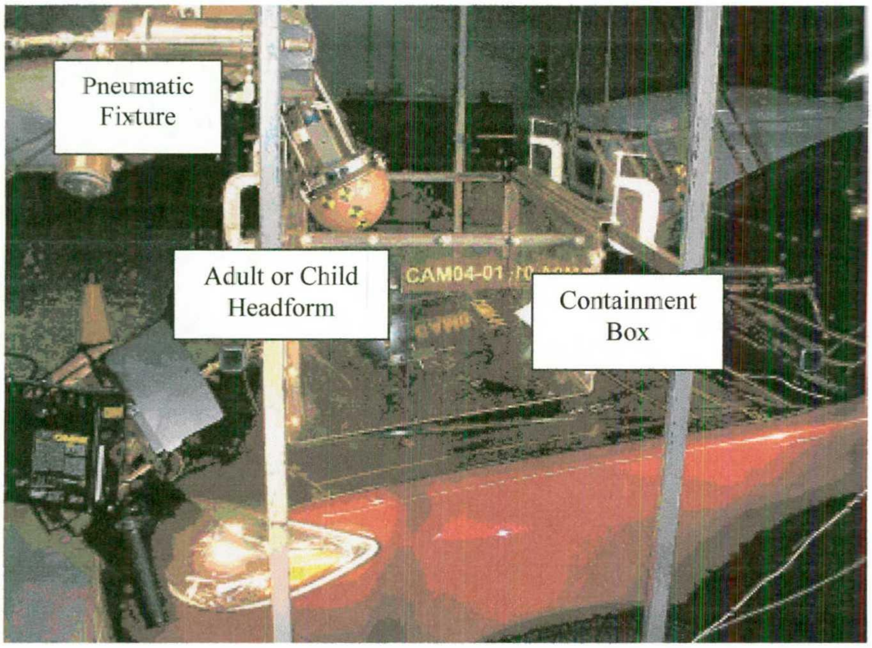

Figure 5: Test Configuration for Vehicle Impacts

The simulation was set up with the headform model a distance of 5 mm above the impacting surface, and the headform was given an impact velocity corresponding to the velocity of the specific test. The surface was given stiffness characteristics that corresponded to impact test data collected at each vehicle impact location represented and a constant acceleration field was given to the headform model to represent the effect of gravity on the system.

In order to determine the stiffness values for the simulated vehicle tests, the acceleration time histories for each test were integrated twice to get deflection (position). The headform resultant acceleration was then multiplied by the mass of the headform to get force. This provided the force-deflection curve that would be give the material characteristics of the impact surface for the MADYMO simulation.

Since the force-deflection curve was determined using the acceleration time history, the correct maximum deflection had to be determined and the rest of the curve truncated. This truncation was done in order to avoid any integration errors from distorting the deflection curve. To avoid these errors, each curve was started at time ‘zero’ (time of impact) and truncated after the total amount of dynamic deflection as measured in the test was reached. After the force-deflection curve was defined, a high order polynomial was fitted to the deflection-time curve using Matlab. The second derivative of the resulting polynomial was then plotted against the original acceleration curve to determine its accuracy. This process was a check to see the effect of the integration error on the data.

The point where the force-deflection curves were truncated proved to be significant since MADYMO would set this point as the point were the headform would stop decelerating and start accelerating in the opposite direction (the point of maximum deflection). To determine the point where the curve was to be truncated, each vehicle impact force-deflection curve was integrated in Matlab to determine the potential energy of each impact using the same cumulative trapezoidal method that was used to integrate the acceleration curves. These values were then compared to the total kinetic energy (6) of the headform at the moment just before impact. The corresponding potential energy that equaled this kinetic energy determined the point where the force-deflection curve was truncated. The equation used to determine the kinetic energy is shown in the following equation:

$$KE = \frac{1}{2} m v^2 \tag{6}$$

KE = Kinetic energy of the headform immediately before impact

m = mass of the headform

v = impact velocity of the headform

Knowing that the total kinetic and potential energies would be equivalent, the potential and kinetic energies are then related using equation (7). The relation was then solved for ‘x’, the maximum displacement.

$$\begin{aligned} KE = PE = \frac{1}{2} m v^2 = \frac{1}{2} k x^2 \\ x = \sqrt{\frac{m v^2}{k}} \end{aligned} \tag{7}$$

PE = Potential energy absorbed by the vehicle structure

k = Stiffness of vehicle structure

x = displacement of vehicle structure

2.2 Case Reconstructions

The second major part of this study focused on injuries to the brain itself, specifically the injuries that are predicted by SIMon. Through in depth study of selected cases in the PCDS, potential correlations between brain injury and vehicle parameters were proposed. These potential correlations were then tested against the entire number of pertinent PCDS cases to develop statistically viable conclusions.

Ten cases were chosen from the PCDS database and reviewed (Table 2). In attempting to reconstruct the kinematics of the cases, particular care was given to mimicking the striking vehicles' profile, the pedestrians' size and weight, the speed of impact, and other relevant parameters. The material characteristics of the bumper for each of the simulations were approximated using a linear stiffness value of 300 kN/m, which provided enough rigidity to provide an accurate response in the pedestrian model. In the case where the hood stiffness had to be approximated, previous impact tests of similar vehicles were used to provide the necessary force-deflection curves.

Case #	Vehicle Model/Year	Age/Gender	Height (cm)/Weight (kg)	MAIS(Head)
1	Plymouth Sundance/1994	6/male	102/20	5
2	Dodge Ram/1996	47/male	165/57	4
3	Toyota Celica/1989	8/female	138/62	2
4	Plymouth Voyager/1992	55/male	183/83	1
5	Ford F150/1994	42/male	168/50	5
6	Ford Taurus/1996	48/male	178/82	2
7	Honda Civic/1993	13/male	152/43	5
8	Chevrolet Cavalier/1996	25/female	170/60	5
9	Honda Civic/1990	33/female	150/57	3
10	Honda Civic/1990	47/male	196/98	3

Table 2: List of PCDS Cases reconstructed

Although care was taken to accurately simulate these parameters, the current reconstructions are based on data gathered by police, medical personnel and witnesses at the scene after the event; hence there is human error built into the reconstructions based on individual accounts of the accident. Because of the uncertainty in the case documentation, the primary measure in this study for determining the accuracy of the simulation involved use of the SIMon algorithm to predict the probability of specific brain injuries suffered in each case. The probability of injury was then compared with whether or not those injuries were sustained in each case. If the individually reported brain injuries and their severities matched the SIMon-predicted probabilities of those injuries, the reconstruction was deemed to be a reasonably accurate representation of the case as it was documented. The accuracy of the simulation therefore reflects both the ability of SIMon to predict injury, as well as the ability of the MADYMO and headform models to model the dynamics of the impact based on available case information.

The MADYMO reconstructions contained profiles with varying degrees of detail of the vehicles involved in each case. The lack of a complete set of detailed physical vehicle profiles is due to a variety of reasons such as time, money, and resource availability. Among the PCDS cases selected for in-depth review, several did not include a very detailed geometric vehicle model. Digital mapping of surrogate vehicles of the same make and model was completed using a FARO arm (Model G1202 Rev. 4.6, FARO Technologies Inc., Lake Mary FL), a position-recording device. This technique is shown in Figure 6. Through the use of transformation matrices, the FARO arm is able to determine the location of a point in space relative to a predefined coordinate system. The front profile of each vehicle was mapped out with a grid pattern of desired points, approximately 50 mm apart. However, this spacing changed around certain contours as appropriate in order to obtain the specific details of each profile. The resulting data points were imported into Hypermesh® (Version 6.0, Altair, Troy MI) and then integrated into a three-dimensional object for use in MADYMO. Due to the lack of availability of certain vehicles, some of the profiles were approximated using measurements provided from the PCDS.

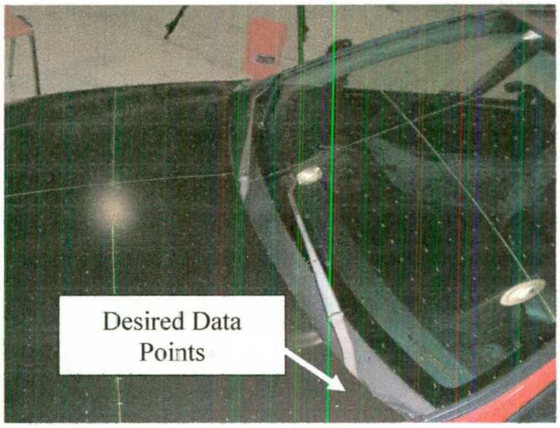

Figure 6: FARO Arm and Vehicle (Left), Grid Guide Pattern for Mapping (Right)

For each of these ten reconstructed cases, MADYMO calculated accelerations at locations within the pedestrian model's head consistent with the accelerometer locations found in a nine-accelerometer array-equipped head of the particular dummy model approximating the size of the case pedestrian. Figure 7 shows a 6-year-old dummy head outfitted with 15 accelerometers. Although accelerations could be measured at each of these locations, only the front, top, side and CG locations were used in a 3-2-2-2 pattern.

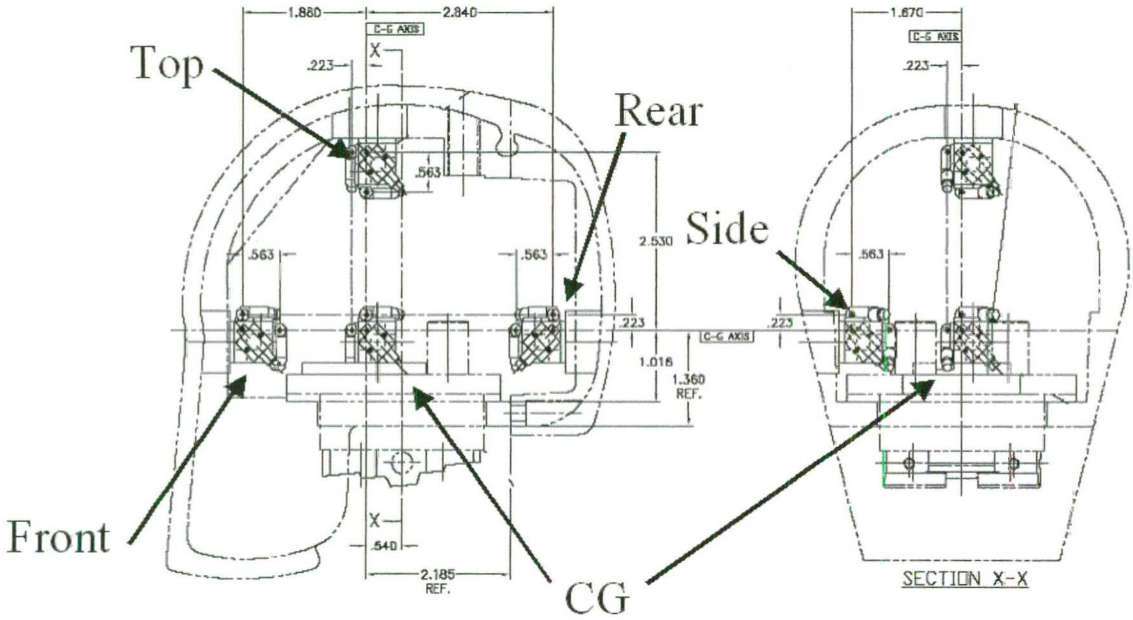

Figure 7: Example of accelerometer locations (Six-year-old dummy head)

The resulting linear accelerations calculated at these points were input into the SIMon algorithm to obtain the rotational accelerations and predict the risk of brain injuries that would occur as a result of the head impacting the vehicle. An additional criterion for measuring the accuracy of each of the MADYMO reconstructions was comparing both the longitudinal wrap around distances (WAD) and the lateral distances between the vehicle centerline and the head impact point to those respective distances measured on the accident case vehicle. The WAD and lateral displacement of the simulated dummy head were measured in each of the reconstructions. Each reconstruction was started at the time of initial impact and the initial vertical impact point was matched to the corresponding point on the model as reported in the case injury list. Impact tests done at the known head impact locations provided the necessary stiffness input for the simulation. These headform to vehicle impact tests were done at impact velocities approximating the accident situation.

As another means of deciding if a particular reconstruction accurately depicted a case impact, a point system was devised to grade each simulation. This point system gave low scores to reconstructions that did not accurately predict the injuries that occurred in the case while giving high scores to reconstructions that accurately predicted the injuries observed in the accident. This system evaluated the combined performance of the MADYMO simulation, the IHRA headform model, the SIMon injury prediction algorithm, and the HIC. Table 3 shows the point values given for every reconstruction prediction. Further, the point system would also provide a tool to compare how prediction tools for different injury types worked in comparison to one another.

Rating	Points Assigned
Good (0 - 25%: No Injury, 75 - 100%: Injury)	3
Fair (25 - 50%: No Injury, 50 - 75%: Injury)	2
Marginal (50 - 75%: No Injury, 25 - 50%: Injury)	1
Poor (75 - 100%: No Injury, 0 - 25%: Injury)	0

Table 3: Point System

An example of how the point system works is as follows. If a contusion was reported in the case and SIMon predicted an 86% chance of a contusion, that particular prediction would get a 'good' rating and receive three points. Similarly, if a contusion was not reported in the case and SIMon predicted a 12% chance of a contusion, this would also get a 'good' rating and receive three points. If there was no reported contusion and SIMon predicted a 78% chance of contusion, this injury prediction would get a 'poor' rating and no points would be awarded. This process would be repeated for each of the four injuries predicted by SIMon and HIC for a total of twelve possible points per case. Differentiation among AIS levels was not included because SIMon does not differentiate between varying levels of injury, only the probability of a certain injury occurring.

2.2.1 Case #1: Plymouth Sundance into 6-year-old dummy model

This case involved a 1994 Plymouth Sundance traveling northbound on a residential street with a posted speed limit of 40.2 km/h (25 mph). The victim involved in the accident was a six-year-old male, 102 cm tall and weighing 20 kg (44.1 lb). The victim allegedly ran eastbound out from between parked cars on the left side of the street and was struck 30 cm from the centerline of the car on the passenger side. According to the accident report, the driver of the Sundance was estimated to be traveling approximately 30 km/h (18.6 mph) at the time of the accident.

The victim suffered extensive injuries ranging from right lower leg lacerations and avulsions to upper torso burns and abrasions. The most serious injuries, however, came from the right and back of the victim's head striking the edge of the hood, close to the fender. As a result of these injuries to the head, the victim later died. From the accident report, the three injuries that were identified as being directly related to the cause of death were the injuries sustained by the brain including an intraventricular hemorrhage, an 18-hour loss of consciousness with neurodeficit, and diffuse edema. Other head injuries were not directly identified as causes of death, including subarachnoid hemorrhaging. While there were many head injuries sustained, no brain contusions or skull fractures were reported.

In constructing the MADYMO simulation, it was critical to mimic the profile and dimensions of the hood and front bumper of the Plymouth Sundance as well as the initial impact point and the wrap around distance. A simplified model was constructed using measurements of landmarks on the Sundance hood and bumper (Figure 8). The profile of the vehicle was divided into a hood section and bumper section with the appropriate stiffness characteristics given. A Hybrid III 6 year old MADYMO dummy model was used for this simulation and was scaled using the MADYMO scaling module and the known mass, age and height values to match the dimensions of the victim involved.

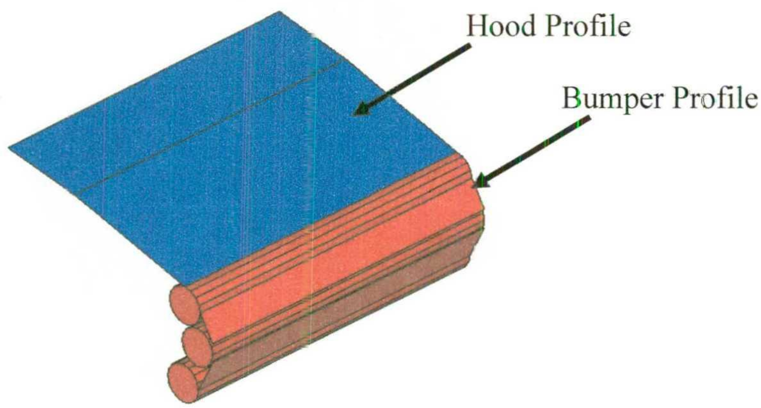

Figure 8: Sundance profile

In order to obtain the correct impact location, the model was offset from the longitudinal centerline of the car by 30 cm at the time of impact based on the case documentation of vehicle damage. The vehicle was given a two-dimensional velocity input such that the pedestrian's velocity perpendicular (lateral) to the direction of travel of the car would be accounted for in the overall kinematics of the collision. The vehicle's longitudinal (x) velocity was set to 36 km/h (22.4 mph) and the lateral (y) velocity was set to 3.13 m/s (7 mph) in order to match the head impact location. The lateral velocity was estimated based on the angle of the vehicle damage in the case so that the pedestrian would strike the vehicle at the correct lateral location.

2.2.2 Case #2: Dodge Ram into 50th percentile male dummy model

The Dodge Ram case involved a 1996 Dodge Ram 2500 truck traveling southbound in the middle lane of a six lane divided roadway at 64.4 km/h (40 mph). The victim, a 47-year-old male 1.65 m tall weighing 57 kg, (126 lb) was crossing westbound. He stopped on the median barrier before continuing to run across the southbound lanes. The driver locked up the brakes before contacting the right side of the pedestrian approximately 40 cm from the centerline of the vehicle on the passenger side.

The victim's head injuries were moderately severe resulting from occipital head contact on the hood of the vehicle. These head injuries included a bruise above the right ear and a small occipital contusion to the skin as well as a small fronto-parietal subdural hematoma and small frontal brain contusion, AIS 4 and 3 respectively. Although the victim did not remember being hit, a loss of consciousness was not reported. The pedestrian had a blood alcohol level of 0.27, and this was identified as a factor in causing the collision.

For the simulation of the accident, a digitized representation of the profile of the Dodge Ram was constructed using a FARO Arm (Figure 9). The vehicle profile was divided into two parts, the hood/cowl area and the bumper/grill area, with each area given different stiffness characteristics. The bumper structure was assumed to be rigid, that is having a large stiffness value. A Hybrid III 50th percentile standing male dummy MADYMO model was used, scaled to match the dimensions of the victim involved in the accident.

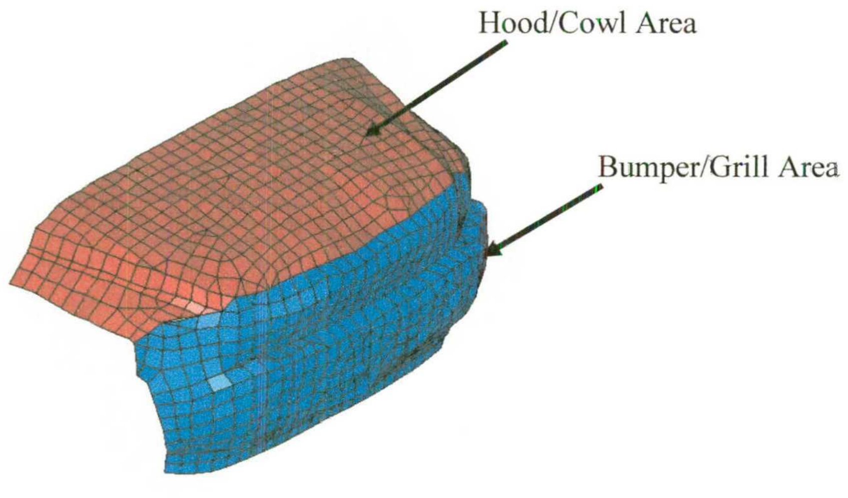

Figure 9: Ram profile

The model was offset from the centerline of the vehicle by 40 cm in accordance with the accident report to achieve the correct striking profile and impact point. The pedestrian's arms and legs were positioned to simulate a jogging stance as well as to have the back of the model's head strike the vehicle to mimic the location of the case head injuries. The vehicle was given a longitudinal (x) velocity of 6.7 m/s corresponding to the reported approximate 24.1 km/h (15 mph) speed at the time of the impact. There was also a lateral (y) velocity of 2 m/s (4.5 mph) given in order to simulate the pedestrian's westbound jogging speed.

2.2.3 Case #3: Toyota Celica into 5th percentile female dummy model

The 'Toyota Celica' case involved a 1989 Toyota Celica traveling southbound in the right lane of a two-lane undivided roadway with a speed limit of 48.3 km/h (30 mph). The victim was an 8 year old female, 1.38 m tall weighing 61.7 kg (136 lb) and was running westbound across the roadway perpendicular to the vehicle. The vehicle contacted the pedestrian near the centerline of the vehicle while traveling at an estimated 40 km/h (26 mph).

Despite the relatively high impact speed, the victim's head injuries were limited, with most of the more serious injuries occurring in the thoracic and lower extremities. These head injuries included a right and left cheek contusion and an abrasion to the lip as well as a reported three-minute loss of consciousness with amnesia (AIS 2). The most severe injuries were to the right leg and consisted of an open proximal tibia fracture and fibula fracture (AIS 3 and 4 respectively).

Again, a digitized representation of the profile of the Toyota Celica was constructed using a FARO Arm (Figure 10). A Hybrid III 5th percentile female dummy MADYMO model was used and scaled to match the victim's height and weight.

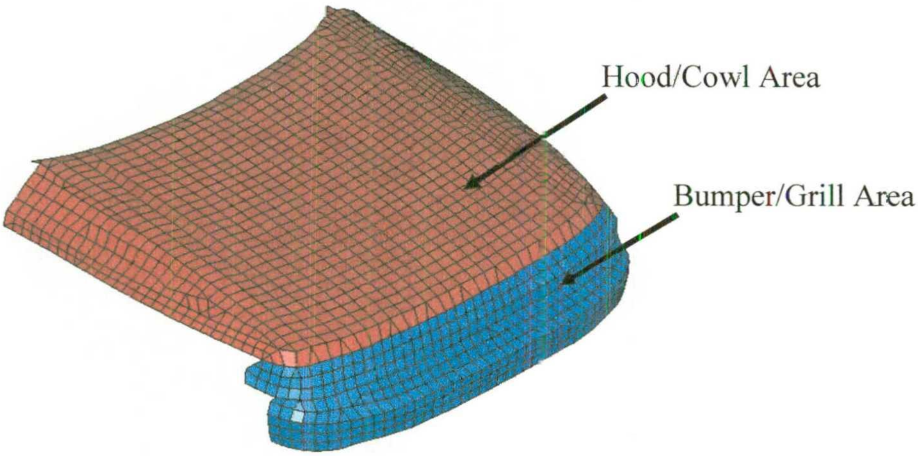

Figure 10: Celica profile

The model was placed at the centerline of the vehicle in accordance with the accident report. The pedestrian's arms and legs were positioned in such a way to simulate a running stance as well as to have the face of the model strike the vehicle when the simulation was run. The vehicle was given a longitudinal (x) velocity of 11.8 m/s corresponding to the reported approximate 41.8 km/h (26 mph) speed at the time of the impact. There was also a lateral (y) velocity of 3.6 m/s (8.1 mph) given in order to simulate the pedestrian's westbound running speed.

2.2.4 Case #4: Plymouth Voyager into 50th percentile male dummy model

This case involved a 1992 Plymouth Voyager traveling northbound on a residential street with a posted speed limit of 56.3 km/h (35 mph). The victim involved in the accident was a 55 year old male, 183 cm tall and weighing 82.6 kg (182 lbs). The victim was jogging northbound on the side of the street when the car struck him from behind, 53 cm from the centerline of the car on the passenger side. According to the accident report, the driver of the Voyager was estimated to be traveling about 28.0 km/h (17.4 mph) at the time of the accident and executed no avoidance maneuvers.

The victim suffered extensive but mostly surface injuries ranging from right lower leg contusions and abrasions to upper torso contusions and abrasions. The most serious injuries came from the back of the victim's head striking the windshield of the vehicle. As a result of this impact, the victim suffered a hematoma to the right occiput, AIS 1. Although there was no loss of consciousness reported, the victim reported that he did not know what hit him and felt dizzy after the accident.

In constructing the simulation, it was again critical to mimic the profile and dimensions of the windshield, hood and front bumper of the Plymouth Voyager as well as the initial impact point and the wrap around distance. A simplified model was constructed using measurements of landmarks on the Voyager windshield, hood and bumper (Figure 11). The profile of the vehicle was divided into a windshield section, hood section and bumper section with the appropriate stiffness characteristics given to each. As before, the bumper was assumed to be a rigid body while the windshield stiffness characteristics was determined from impact testing. A Hybrid III 50^{th} percentile MADYMO dummy model was used for this simulation and was scaled to match the dimensions of the victim involved.

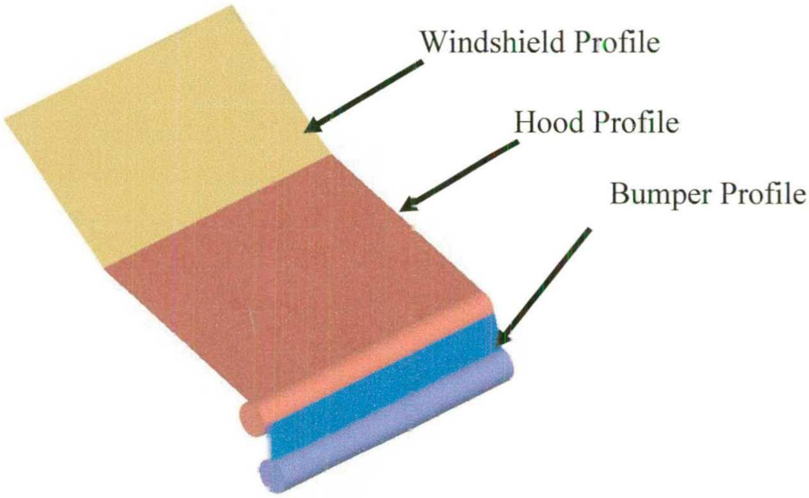

Figure 11: Voyager profile

In order to obtain the correct impact location and to stay consistent with the case description, the model was offset from the longitudinal centerline of the car by 50 cm at the time of impact. The vehicle's longitudinal (x) velocity was set to 28.0 km/h (17.4 mph) with no lateral velocity given since the pedestrian was moving with the direction of the vehicle and there were no avoidance maneuvers.

2.2.5 Case #5: Ford F150 into 50^{th} percentile male dummy model

The 'Ford F150' case involved a 1994 Ford F150 truck traveling southbound in the left lane of a six lane divided roadway at 56.3 km/h (35 mph). The victim was a 42 year old male, 1.68 m tall weighing 50.3 kg (111 lb), and was crossing eastbound when he stopped and turned to face the oncoming vehicle. The driver locked up the brakes before contacting the front of the pedestrian approximately 52 cm from the centerline of the vehicle on the passenger side.

The victim's head injuries were severe as a result of the head and face striking the hood of the vehicle. These head injuries included an AIS 3 orbital plate fracture, AIS 3 frontal edema to both the left and right side of the brain, extensive AIS 5 shear injuries to the brain, and a large AIS 4 parietal contusion with a loss of consciousness reported. The victim died as a result of these injuries. Further, the presence of both alcohol and cannabinoid in the pedestrian's blood were reported as possible factors in the accident.

For the simulation of the accident, a digitized representation of the profile of the Ford F150 was constructed using a FARO Arm (Figure 12). The vehicle profile was divided into three parts, the hood/cowl area, the hoodguard area, and the bumper/grill area, each with given different stiffness characteristics. The bumper and hoodguard structure were assumed to be rigid while the hood stiffness characteristics were determined by impact testing. A Hybrid III 50th percentile standing male dummy MADYMO model was used in this reconstruction. Again, the simulation model was scaled to match the dimensions of the victim involved in the accident.

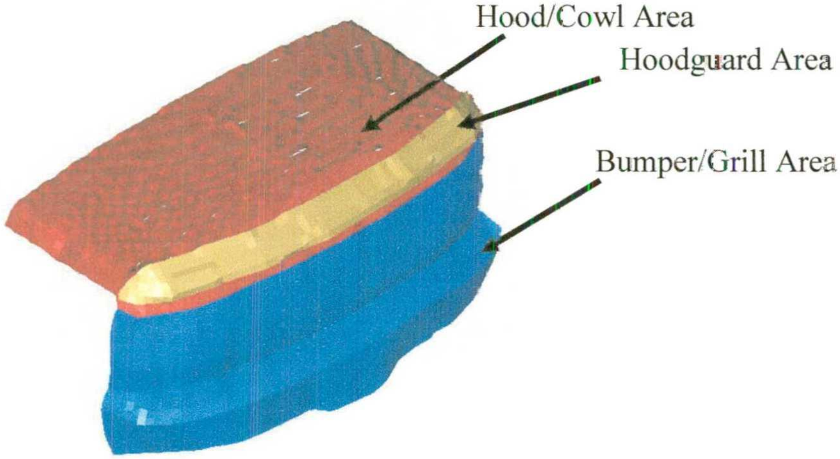

Figure 12: Ford F150 profile

The model was offset from the centerline of the vehicle by 50 cm in accordance with the accident report to achieve the correct striking profile. The pedestrian's arms and legs were positioned to simulate the reported position of the victim facing the oncoming vehicle. The vehicle was given a longitudinal (x) velocity of 8.9 m/s corresponding to the reported approximate 32.2 km/h (20 mph) speed at the time of the impact due to braking. There was no lateral velocity given since the report stated that the pedestrian had stopped and turned to face the oncoming vehicle prior to impact.

2.2.6 Case # 6: Ford Taurus into 50th percentile male dummy model

This case involved a 1996 Ford Taurus traveling northbound on a two-lane roadway with a posted speed limit of 48.3 km/h (30 mph). The victim involved in the accident was a forty eight year old male, 178 cm tall and weighing 81.6 kg (180 lbs). The victim was walking northeasterly across the lanes of travel when the vehicle struck him on the right side and slightly from behind, approximately at the centerline of the vehicle. According to the accident report, the driver of the Taurus locked up the brakes before impact and was estimated to be traveling about 27 km/h (16. 8 mph) at the time of the accident.

The victim suffered few injuries from the impact with the most serious injuries coming from the back of the victim's head striking the windshield of the vehicle. As a result of this impact, the victim suffered a scalp contusion to the left temple (AIS 1) and a one-hour loss of consciousness (AIS 2). The only other injuries reported included a minor right wrist abrasion (AIS 1).

In constructing the simulation, it was critical to mimic the dimensions of the windshield, in addition to the hood and front bumper of the Ford Taurus as well as the initial impact point and the wrap around distance. A simplified model was constructed using measurements of landmarks on the Taurus windshield, hood and bumper (Figure 13). The profile of the vehicle was divided into a windshield section, hood section and bumper section with the windshield stiffness being derived from experimental testing and the hood and bumper given approximate linear stiffness characteristics. A Hybrid III 50^{th} percentile MADYMO dummy model was used for this simulation and was scaled to match the dimensions of the victim involved.

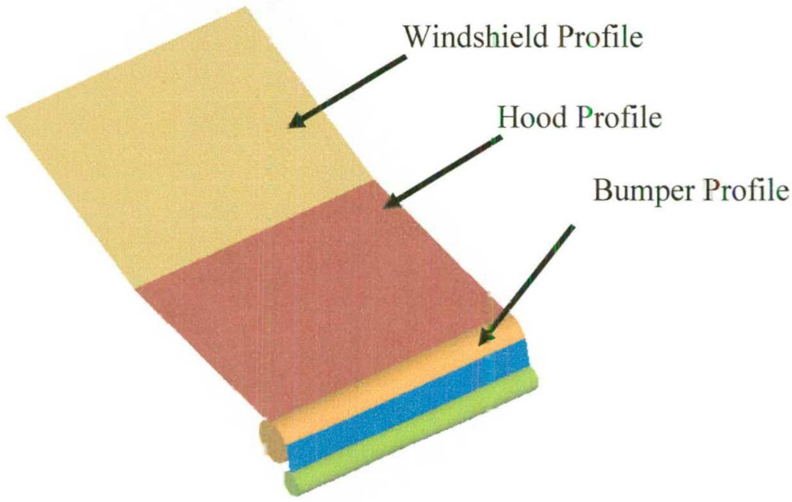

Figure 13: Taurus profile

In order to obtain the correct impact location, the model was placed at the centerline of the car at the time of impact. The vehicle was given a velocity input such that the pedestrian's velocity with the direction of travel of the car would be included in the overall kinematics of the collision. The vehicle's longitudinal (x) velocity was set to 27 km/h (16.8 mph) and lateral (y) velocity was set to 2.0 m/s (4.5 mph).

2.2.7 Case # 7: Honda Civic Coupe into 50th percentile male dummy model

This case involved a 1993 Honda Civic coupe traveling northwest on a three-lane roadway in the right lane with a posted speed limit of 64.4 km/h (40 mph). The victim involved in the accident was a 13 year old male, 152 cm tall and weighing 43.1 kg (95 lbs). The victim was running northeasterly across the lanes of travel when the vehicle struck him on the right side, approximately 45 cm from the centerline of the vehicle. According to the accident report, the driver of the Civic was estimated to be traveling about 38 km/h (23.6 mph) at the time of impact with no avoidance actions recorded.

The victim suffered several injuries from the impact with the most serious injuries resulting from the right side of the victim's head striking the windshield of the vehicle. The victim suffered a fracture to the temporal parietal occipital and petrous bones (AIS 3) as well as extensive edema and shearing (AIS 5), subdural hematoma (AIS 4), temporal contusions (AIS 3) and a loss of consciousness from which the victim never recovered (AIS 5). The victim died as a result of these injuries.

For the simulation of the accident, a digitized representation of the profile of the Honda Civic was constructed using a FARO Arm (Figure 14). The profile of the vehicle was divided into a windshield section, hood section and bumper section with the appropriate stiffness characteristics given to each. A Hybrid III 50th percentile MADYMO dummy model was used for this simulation and was scaled to match the dimensions of the victim involved.

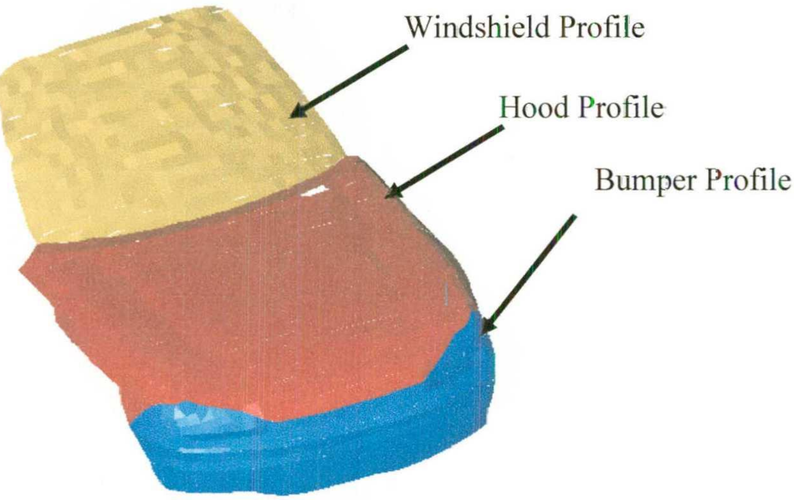

Figure 14: Civic coupe profile

In order to obtain the correct impact location, the model was placed at the centerline of the car at the time of impact. The vehicle was given a velocity input such that the pedestrian's velocity with respect to the direction of travel of the car would be included in the overall kinematics of the collision. The vehicle's longitudinal (x) velocity was set to 39.6 km/h (24.6 mph) and lateral (y) velocity was set to 13.1 km/h (8.2 mph).

2.2.8 *Case # 8: Chevrolet Cavalier into 5th percentile female dummy model*

This case involved a 1996 Chevrolet Cavalier traveling southbound in the middle lane with a posted speed limit of 72 km/h (45 mph). The victim involved in the accident was a thirtythree year old female, 170 cm tall and weighing 60 kg (130 lbs). The victim was running east to west across the lanes of travel when the vehicle struck her on the right side, approximately at the centerline of the vehicle. According to the accident report, the driver of the Cavalier was estimated to be traveling about 67 km/h (41.6 mph) at the time of the impact with no avoidance actions recorded.

The victim suffered several injuries from the impact with the most serious injuries resulting from the victim's head striking the windshield of the vehicle. The victim suffered midbrain swelling and epidural hematoma as well as subarachnoid hemorrhaging (AIS 5) along with suffering a coma (AIS 5). The victim died as a result of these injuries.

For the simulation of the accident, a digitized representation of the profile of the Chevrolet Cavalier was constructed using a FARO Arm (Figure 15). The profile of the vehicle was divided into a windshield section, hood section and bumper section with the appropriate stiffness characteristics given to each. A Hybrid III 50th percentile MADYMO dummy model was used for this simulation and was scaled to match the dimensions of the victim involved.

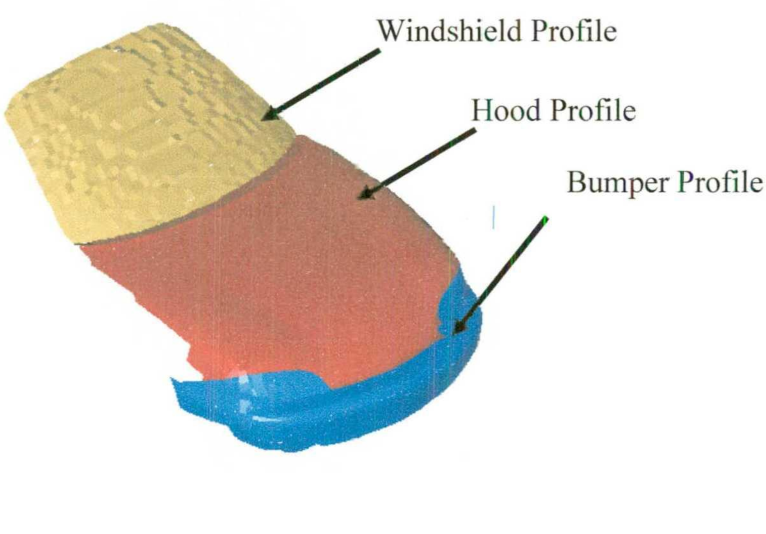

Figure 15: Cavalier profile

In order to obtain the correct impact location, the model was placed at the centerline of the car at the time of impact. The vehicle was given a velocity input such that the pedestrian's velocity with the direction of travel of the car would be included in the overall kinematics of the collision. The vehicle's longitudinal (x) velocity was set to 67.0 km/h (41.6 mph) and no lateral velocity set.

2.2.9 Case # 9: Honda Civic Hatchback into 5th percentile female dummy model

This case involved a 1990 Honda Civic hatchback traveling southbound on a two-lane, one-way roadway in the left lane with a posted speed limit of 48.3 km/h (30 mph). The victim involved in the accident was a twenty five year old female, 150 cm tall and weighing 57 kg (125 lbs). The victim was running southeasterly across the lanes of travel when the vehicle struck her mostly from behind, approximately 31 cm from the centerline of the vehicle on the passenger side. According to the accident report, the driver of the Civic was estimated to be traveling about 32 km/h (19.9 mph) at the time of the impact and locked up the brakes prior to impact.

The victim suffered several injuries from the impact with the most serious injuries coming from the back of the victim's head striking the windshield of the vehicle. As a result of this impact the victim suffered a fracture to the temporal parietal bone (AIS 2), as well as a small temporal contusion to the right side of the brain (AIS 3).

For the simulation of the accident, a digitized representation of the profile of the Honda Civic was constructed using a FARO Arm (Figure 16). Impact tests done on the windshield of the Civic at the known head impact location provided the necessary stiffness input for the simulation. A Hybrid III 50^{th} percentile MADYMO dummy model was used for this simulation and was scaled to match the dimensions of the victim involved.

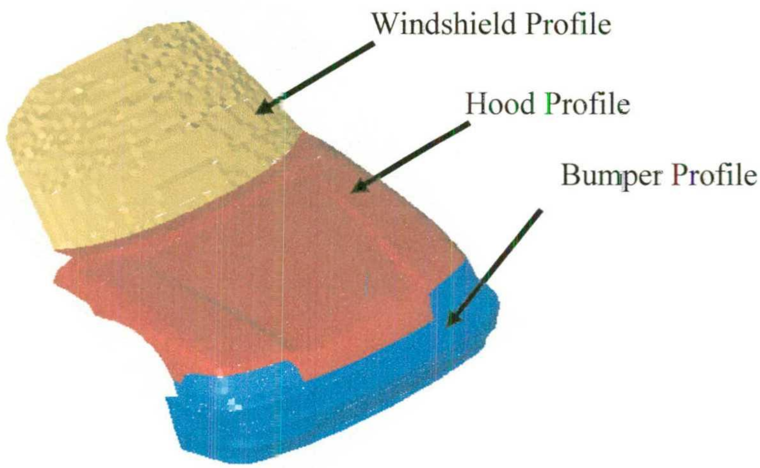

Figure 16: Civic hatchback profile

In order to obtain the correct impact location, the model was placed at the centerline of the car at the time of impact, the case file indicating this being the point where the car impacted the pedestrian. The vehicle was given a velocity input such that the pedestrian's velocity with the direction of travel of the car would be included in the overall kinematics of the collision. The vehicle's longitudinal (x) velocity was set to 32.0

km/h (19.9 mph) and lateral (y) velocity was set to 10.8 km/h (6.7 mph).

2.2.10 Case # 10: Honda Civic Sedan into 50th percentile male dummy model

This case involved a 1990 Honda Civic sedan traveling southbound on a four-lane roadway in the inside lane with a posted speed limit of 40.2 km/h (25 mph). The victim involved in the accident was a forty seven year old male, 196 cm tall and weighing 98 kg (220 lbs). The victim was walking westbound across the lanes of travel when he evidently stopped to drink a beer. The vehicle struck him on the right side, approximately 7 cm from the centerline of the vehicle on the driver's side. According to the accident report, the driver of the Civic was estimated to be traveling about 31 km/h (19.3 mph) at the time of the impact with no avoidance actions recorded.

The victim suffered several injuries from the impact with the most serious injuries resulting from the right side of the victim's head striking the windshield of the vehicle. The victim suffered bifrontal lobe contusions (AIS 3) and a loss of consciousness (AIS 2) as a result of the impact.

Since both the Civic sedan and hatchback were from the same model year, the previous mapping from Case #9 was used (Figure 16). Similarly, the previous stiffness curve derived from the windshield impact was used, with the windshield stiffness considered the same over its entire surface. As before, the profile of the vehicle was divided into a windshield section, hood section and bumper section with the appropriate stiffness characteristics given to each. A Hybrid III 50^{th} percentile MADYMO dummy model was used for this simulation and was scaled to match the dimensions of the victim involved.

In order to obtain the correct impact location, the model was placed at the centerline of the car at the time of impact. The vehicle was given a velocity input such that the pedestrian's velocity with the direction of travel of the car would be included in the overall kinematics of the collision. The vehicle's longitudinal (x) velocity was set to 37.1 km/h (23 mph) with zero lateral velocity. The simulation was started at the time of initial impact and the initial vertical impact point was matched to the corresponding point on the model as reported in the injury list.

Further, through varying particular parameters in the reconstructions, such as bumper height, impact speed, etc. the affect of changes on geometry on injury prediction was observed. Through this analysis, five parameters were chosen as possible correlates to injury: vehicle speed, pedestrian height, bumper height, front-to-top transition point, and hood length. However, since these possible correlates to injury were only based on ten reconstructions, it was determined that further investigation of these parameters was necessary.

2.3 Statistical Analysis of the PCDS

After the ten reconstructions were completed, the results were analyzed to determine if there were any apparent trends in the data or correlations between the various parameters listed in the cases and the resulting injuries. To determine the various parameters that would be investigated, the simulations were varied slightly to determine the effect and sensitivity of the physical parameters (for example; bumper height, pedestrian height, impact speed) on the SIMon-predicted injuries. To help narrow the field of parameters that would be investigated, only those parameters that would be expected to influence the pedestrian impact position and head impact velocity were considered, drawing on the knowledge gained from the reconstructions.

Through this analysis, five parameters were chosen as possible correlates to injury: vehicle speed, pedestrian height, bumper height, front-to-top transition point, and hood length. The various parameters are self-explanatory with the exception of the front-to-top transition point. This point was defined as the wrapping (following the contour of the bumper) distance to the point at which, in the process of measuring the WAD, the distance measured changed from a vertical (upwards from the road surface) distance to a longitudinal (along the hood) distance (i.e. the point at which the pedestrian would begin to pivot).

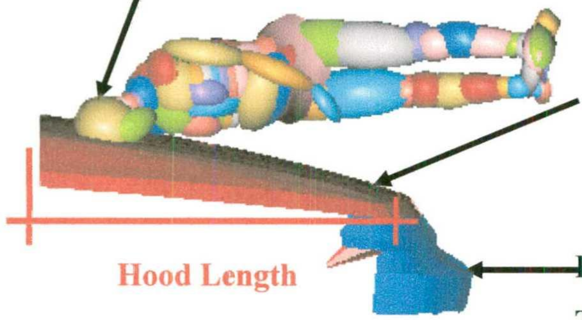

Figure 17: The four vehicle geometry parameters + Pedestrian Height investigated

Although originally all five parameters were to be examined, bumper height and hood length were later taken out of the analysis since it was determined through statistical analysis that neither was strongly correlated with WAD. This deletion left the vehicle speed, pedestrian height, and the front-to-top transition point as the primary parameters of interest.

These three independent parameters were then correlated to the occurrence of head injuries in the PCDS cases. The comparison was done using a multiple logistic regression analysis in SAS statistical software (SAS 9.1, The SAS Institute, Cary, NC, USA). Logistic regression was used for the correlations that involved injury because the dependent variables only had two values (injury or non-injury). Each of these logistic regressions looked at the injuries that were predicted by SIMon and HIC (ASDH, DAI, contusions and skull fracture) as well as any head injury of AIS 3 and AIS 2 or above. If a correlation were found, SAS would produce two numbers, an intercept and a parameter estimate. Injury probability curves as a function of each independent parameter were generated based on equation (8).

$$\ln(z) = x + w \cdot y \tag{8}$$

z = event of interest

x = intercept estimate

w = geometry parameter that is to be varied

y = parameter estimate

The resulting odds at each value of 'w' were calculated using equation (9).

$$Odds = e^{\ln(z)} \tag{9}$$

z = event of interest

$Odds$ = odds of event occurring

Finally, the probability of injury occurring given the geometry parameter varied was calculated using equation (10).

$$P = \frac{Odds}{Odds + 1} \tag{10}$$

P = Probability of event (injury/non-injury) occurring

$Odds$ = odds of event occurring

These calculations were done in Excel and the resulting probability curves plotted for values of the parameter that are relevant to general impact situations. In addition to this multiple logistic regression analysis, correlations that did not include binary dependent variables were carried out using multiple regression analysis. These relations that did not fit the logistic (injury or no injury) criteria and that were also found to have a correlation according to SAS were plotted according to equation (11).

$$A = b_0 + x_1 b_1 + x_2 b_2 + \ldots \qquad (11)$$

A = dependent variable that was determined to be a function of parameter 'x'

x_n = independent parameter that is to be varied were n=1,2,3…

b_0 = Intercept estimate given by SAS

b_n = parameter estimate given by SAS, where n=1,2,3…

The geometric independent parameter (front-to-top transition point) was normalized by the corresponding pedestrian height. The wrap around distance (WAD) was then examined as a function of the ratio of transition point to pedestrian height. Vehicle speed was used to normalize the resulting head velocity seen in the reconstruction. The ratio of head velocity to vehicle speed was then examined as a function of WAD. Finally, the stiffness of the impact points were examined and plotted to see how stiffness varied as a function of WAD.

CHAPTER 3

RESULTS

3.1 HIC Predictive Algorithm

Table 4 shows the results from the spring tests used to validate the headform model at low speeds and varying stiffness. Table 5 shows the results from the vehicle tests used to validate the model at high speeds and actual vehicle stiffness.

Velocity	12.6 km/h			15.26 km/h			17.60 km/h		
Stiffness	Actual	Model	%	Actual	Model	%	Actual	Model	%
20 kN/m	33	32	1.5	54	53	1.1	74	76	3.4
41 kN/m	56	54	4.8	90	89	1.7	124	127	2.7
198 kN/m	165	172	4.4	266	285	7.2	394	409	3.9

Table 4: Results of head-drop tests (HIC values), Percent difference of model values from experimental values

Test #	2001 Honda Civic			2004 GMC Savana			2001 Ford Escape		
	Actual	Model	%	Actual	Model	%	Actual	Model	%
1	722	723	0.1	581	544	6.4	708	761	7.5
2	683	676	1.0	585	588	0.5	948	976	3.0
3	511	507	0.8	525	501	4.6	1131	1124	0.6
4	965	964	0.1	985	994	0.9	406	435	7.1
5	1005	953	5.2	N/A	N/A	N/A	839	842	0.4
6	N/A	N/A	N/A	N/A	N/A	N/A	1230	1264	2.8
7	N/A	N/A	N/A	N/A	N/A	N/A	2292	2339	2.1
Test #	2003 Dodge Ram			2004 Toyota Camery			2004 Toyota Sienna		
	Actual	Model	%	Actual	Model	%	Actual	Model	%
1	1321	1368	3.6	502	549	9.4	598	618	3.3
2	1193	1204	0.9	508	476	6.3	403	391	3.0
3	555	519	6.5	1701	1701	0.0	1387	1263	8.9
4	614	612	0.3	454	448	1.3	1363	1451	6.5
5	626	626	0.0	733	734	0.1	N/A	N/A	N/A
6	N/A	N/A	N/A	1759	1700	3.4	353	331	6.2

Table 5: Results of vehicle tests (HIC values)

As shown in Table 4, the headform model compares well with the experimental spring drop tests, with very little error, the average percent deviation being 3.4%. This close match confirms the decision to model the impact as an inelastic collision. Table 5 shows the HIC values for the GTR vehicle tests compared with simulation. Again, when comparing the HIC values, we see that the model compared with the experimental results with only a few discrepancies approaching 10 percent, the average percent deviation being 3.2%.

Figure 20 graphically shows the HIC algorithm derived from simulations with the IHRA headform model. As stated before, the linear stiffness values and impact velocity values were varied with each combination of values resulting in a different HIC. The results of the experimental head drops and vehicle impacts are overlaid on the figure to illustrate accuracy of the model as well as illustrating where the U.S. fleet falls in the graph. The red circles represent the experimental head drops while the yellow circles represent the vehicle impacts (GTR tests). Since the corresponding linear stiffness values could not be determined for the GTR tests, the yellow dots were placed by knowing only the impact velocity and resulting HIC value. The HIC predictive algorithm can be expressed generally as (11):

$$\begin{aligned} HIC = 1662 + (-8.9852)x_1 + (-560.37)x_2 \ldots \\ \ldots + (3.1904)x_1 x_2 + (-0.017)x_1^{\ 2} + (41.157)x_2^{\ 2} \end{aligned} \tag{11}$$

HIC = Head Injury Criteria

x_1 = Linear Stiffness (kN/m)

x_2 = Impact Speed (m/s)

Figures 18 and 19 show how this predictive algorithm compares graphically to the data gained from the simulations.

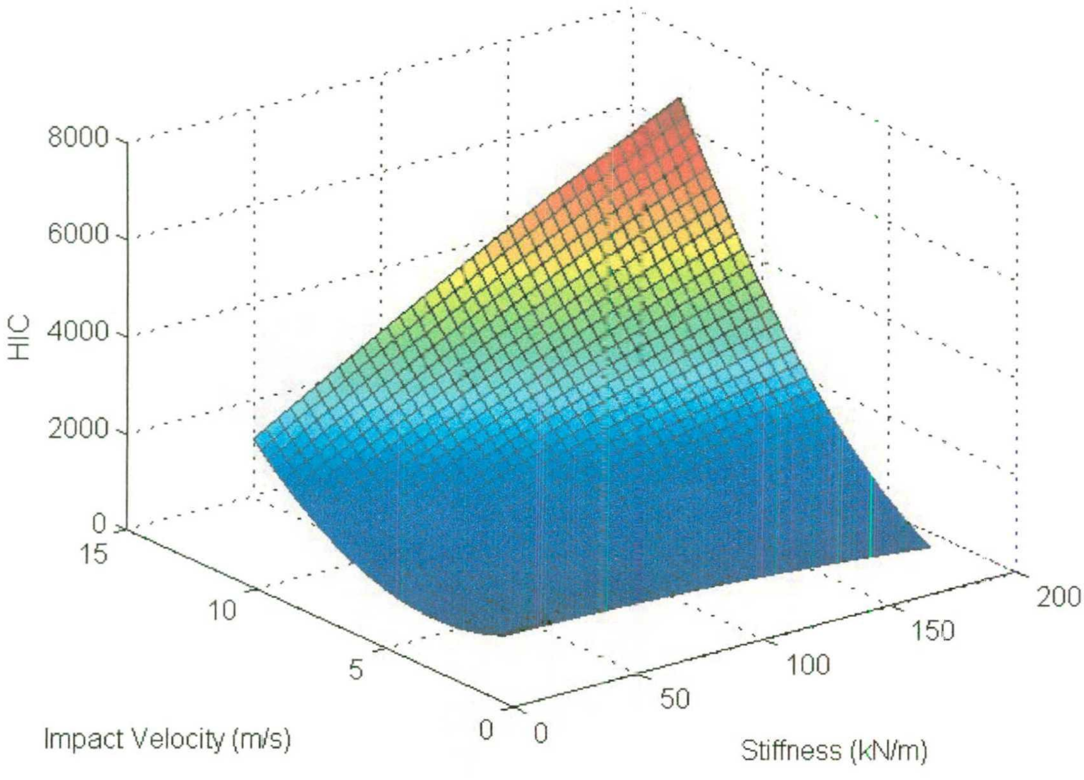

Figure 18: HIC vs. Stiffness vs. Velocity as defined by equation (11)

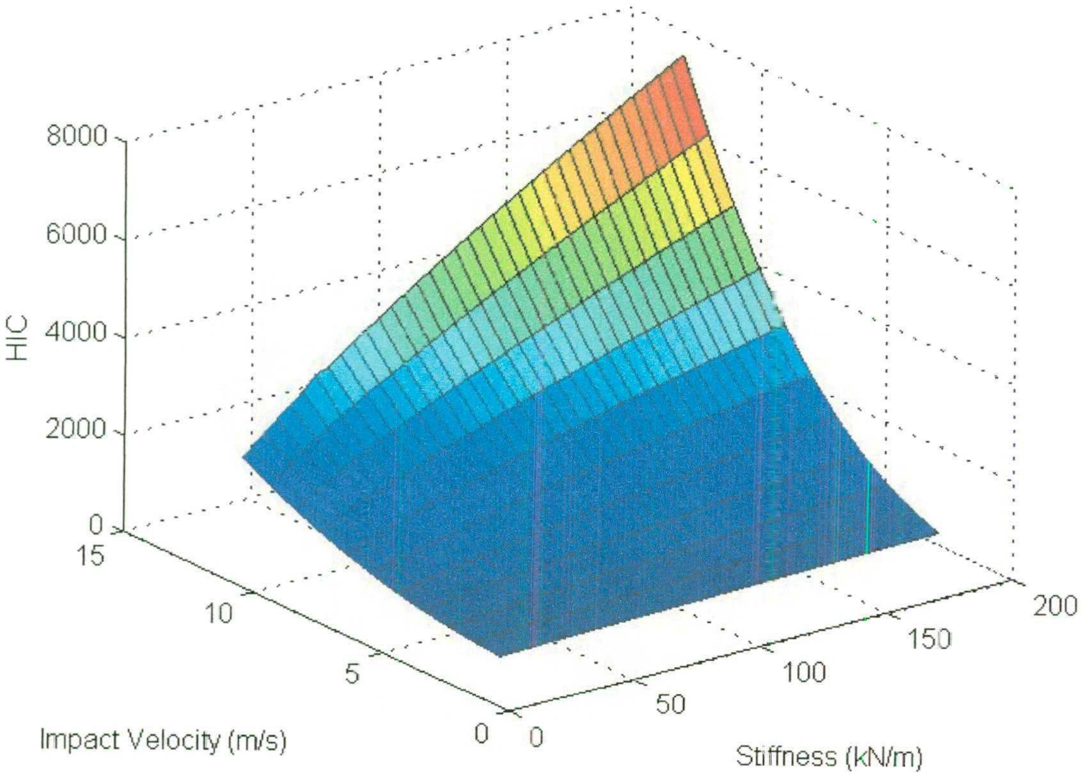

Figure 19: HIC vs. Stiffness vs. Velocity as defined by simulation data

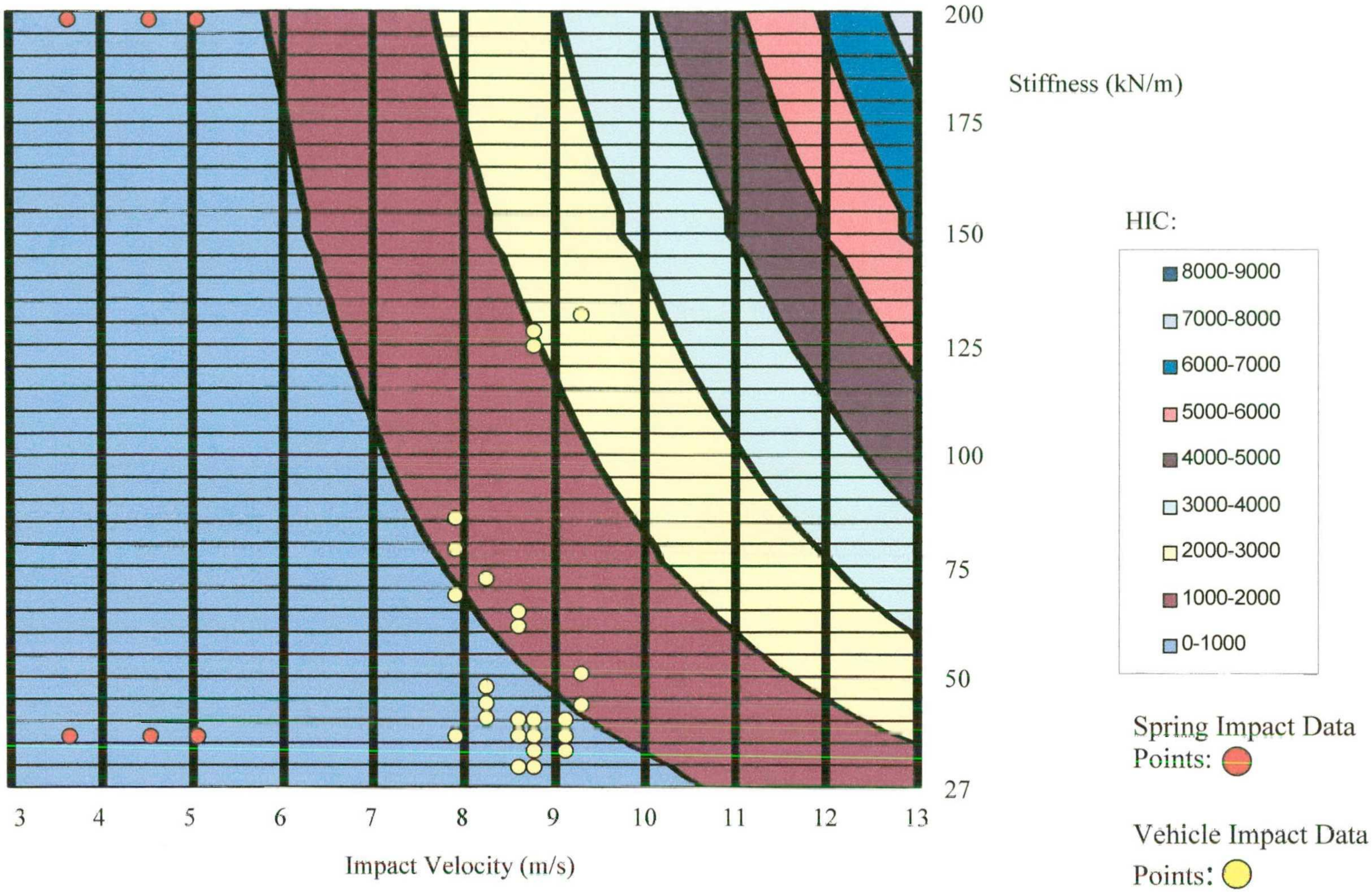

Figure 20: HIC vs. Stiffness vs. Velocity

3.2 Case Reconstructions

For each of the reconstructions, the conditions chosen for the simulation as defined previously lead to a close match with the reported wrap around distance (WAD) and pedestrian-to-vehicle contacts as shown in the following figures. For each of the cases, a figure showing the initial pre-impact position and head impact position is given as well as a table showing the comparison of the simulated impact point to the actual reported impact point.

3.2.1 Case #1: Plymouth Sundance

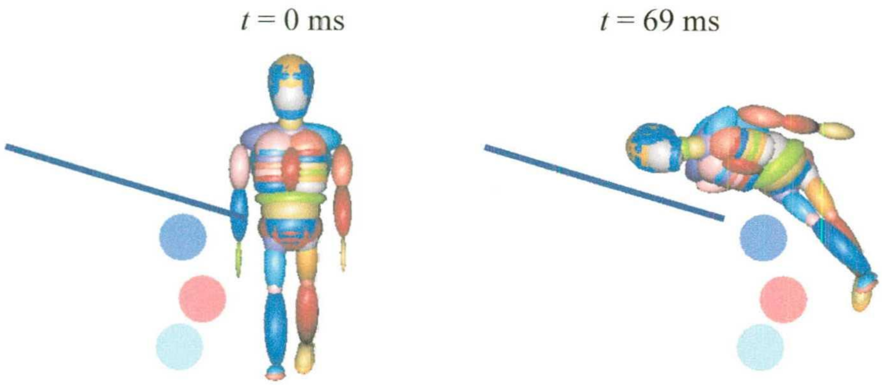

Figure 21: Screen captures from Plymouth Sundance simulation (initial and head contact)

Reported WAD (m)	1.30	Reported Lateral Impact Location (m)	0.60
Simulated WAD (m)	1.35	Simulated Lateral Impact Location (m)	0.56
Percent Difference	3.8%	Percent Difference	6.2%

Table 6: Comparison of the Actual and Simulated (Plymouth Sundance) WAD Values

After the simulation was run and the SIMon algorithm executed, the predicted injuries were compared to the case head injuries. SIMon predicted a 65% chance of a diffuse axonal injury, a 23% chance of a brain contusion, and a 100% chance of an acute subdural hematoma. Further, it predicted a 100% chance of an AIS 3 skull fracture predicted. These predicted injuries all correlated rather well with the actual injuries sustained by the victim, as shown in Table 7.

Case	Simulation
Intraventricular Hemorraging, left side of the brain (AIS 5)	100% Chance ASDH on the left side of the brain (RMDM = 4.81)
Loss of Consciousness (AIS 5)	65% Chance DAI (CSDM (0.15) = 0.650)
No Brain Contusions	23% Chance Contusion (DDM = 0.027)
Fracture of right temporal bone (AIS 2)	100% Chance AIS 3 Skull Fracture (HIC = 3133)

Table 7: Plymouth Sundance Case injury vs. simulation results

3.2.2 Case #2: Dodge Ram

$t = 10$ ms $t = 110$ ms

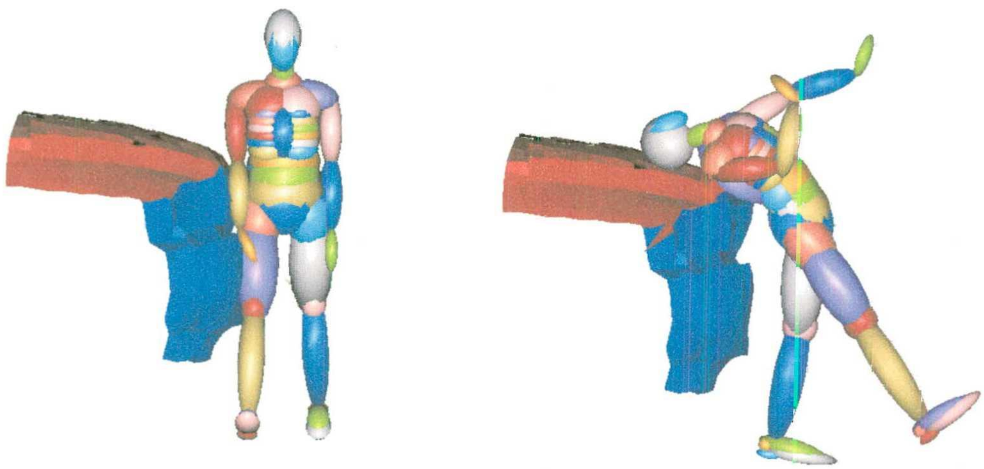

Figure 22: Screen captures from Dodge Ram simulation (initial and head contact)

Reported WAD (m)	1.46	Reported Lateral Impact Location (m)	0.68
Simulated WAD (m)	1.57	Simulated Lateral Impact Location (m)	0.67
Percent Difference	7.4%	Percent Difference	1.7%

Table 8: Comparison of the Actual and Simulated (Dodge Ram) WAD Values

Case	Simulation
Fronto-Parietal Subdural Hematoma on the right side of the brain (AIS 4)	99% Chance ASDH on the right side of the brain (RMDM = 2.21)
No DAI Reported	33% Chance DAI (CSDM = 0.432)
Small Frontal Contusion (AIS 3)	48% Chance Contusion (DDM = 0.069)
No Skull Fractures	4.3% Chance AIS 3 Skull Fracture (HIC = 275)

Table 9: Dodge Ram Case injury vs. simulation results

SIMon predicted a 33% chance of a diffuse axonal injury occurring, a 48% chance of a brain contusion and a 99% chance of an acute subdural hematoma. These predicted injuries, for the most part, correlated well with the actual injuries sustained as seen in Table 9. The prediction of the chance of a contusion gave almost a 50 percent chance of an injury occurring.

3.2.3 Case #3: Toyota Celica

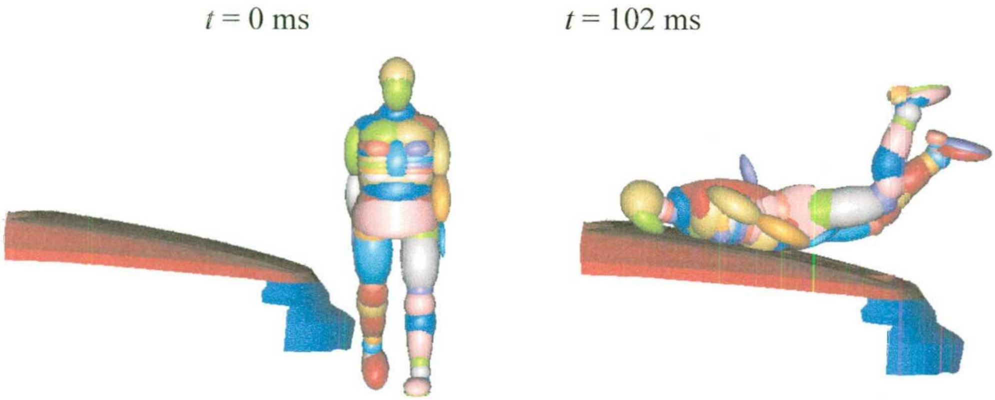

Figure 23: Screen captures from Toyota Celica simulation (initial and head contact)

Reported WAD (m)	1.79	Reported Lateral Impact Location (m)	0.52
Simulated WAD (m)	1.97	Simulated Lateral Impact Location (m)	0.475
Percent Difference	9.9%	Percent Difference	8.6%

Table 10: Comparison of the Actual and Simulated (Toyota Celica) WAD Values

Case	**Simulation**
No Reported Internal Bleeding	40% Chance ASDH on the right side of the brain (RMDM = 0.844)
No DAI Reported	60% Chance DAI (CSDM = 0.602)
No Brain Contusions	10% Chance (DDM = 0.003)
No Skull Fractures	99% Chance AIS 3 Skull Fracture (HIC = 2338)

Table 11: Toyota Celica Case injury vs. simulation results

For this simulation, SIMon predicted a 60% chance of a diffuse axonal injury occurring, a 10% chance of a brain contusion and a 40% chance of an acute subdural hematoma. These predicted injuries, for the most part, correlated well with the actual injuries sustained as seen in Table 11. However, the prediction of the chance of an AIS 3 skull fracture did not correlate well with the reported injuries.

3.2.4 Case #4: Plymouth Voyager

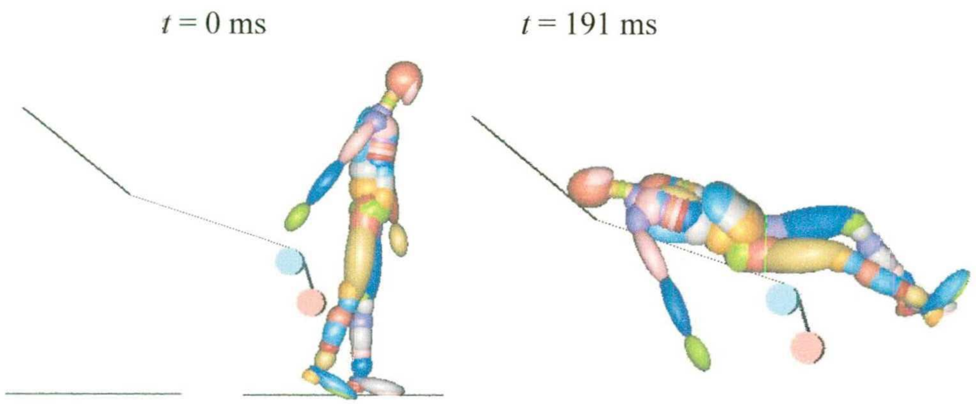

Figure 24: Screen captures from Plymouth Voyager simulation (initial and head contact)

Reported WAD (m)	2.00	Reported Lateral Impact Location (m)	0.52
Simulated WAD (m)	1.95	Simulated Lateral Impact Location (m)	0.51
Percent Difference	2.6%	Percent Difference	2.4%

Table 12: Comparison of the Actual and Simulated (Plymouth Voyager) WAD Values

Case	Simulation
Hematoma to the right occipital bone (AIS 1)	99% Chance ASDH on the left side of the brain (RMDM = 2.24)
No DAI Reported	70% Chance DAI (CSDM = 0.664)
No Contusion Reported	25% Chance Contusion (DDM = 0.032)
No Skull Fractures	29% Chance AIS 3 Skull Fracture (HIC = 740)

Table 13: Plymouth Voyager Case injury vs. simulation results

SIMon predicted a 70% chance of a diffuse axonal injury occurring, a 25% chance of a brain contusion and a 99% chance of an acute subdural hematoma. These predicted injuries, for the most part did not correlate well with the actual injuries sustained as seen in Table 13.

3.2.5 Case #5: Ford F150

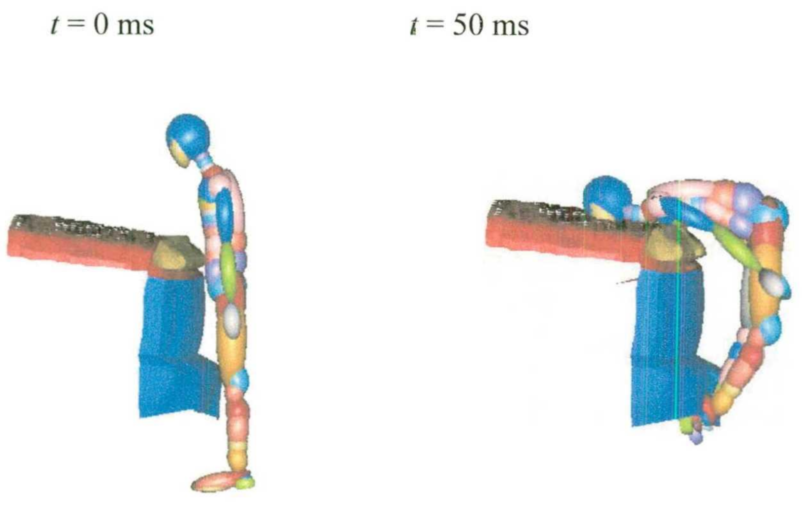

Figure 25: Screen captures from Ford F150 simulation (initial and head contact)

Reported WAD (m)	1.52	Reported Lateral Impact Location (m)	0.56
Simulated WAD (m)	1.45	Simulated Lateral Impact Location (m)	0.54
Percent Difference	4.4%	Percent Difference	3.0%

Table 14: Comparison of the Actual and Simulated (Ford F150) WAD Values

Case	**Simulation**
Extensive Shear Injury (AIS 5)	100% Chance ASDH on the left side of the brain (RMDM = 4.13)
LOC, Frontal Edema (AIS 3)	92% Chance DAI (CSDM = 0.925)
Large Partial Contusion (AIS 4)	60% Chance Contusion (DDM = 0.084)
Orbital Plate Fracture (AIS 3)	97% Chance AIS 3 Skull Fracture (HIC = 1904)

Table 14: Ford F150 Case injury vs. simulation results

SIMon predicted a 92% chance of a diffuse axonal injury occurring, a 60% chance of a brain contusion and a 100% chance of an acute subdural hematoma. These predicted injuries correlated well with the actual injuries sustained by the victim as seen in Table 14.

3.2.6 Case #6: Ford Taurus

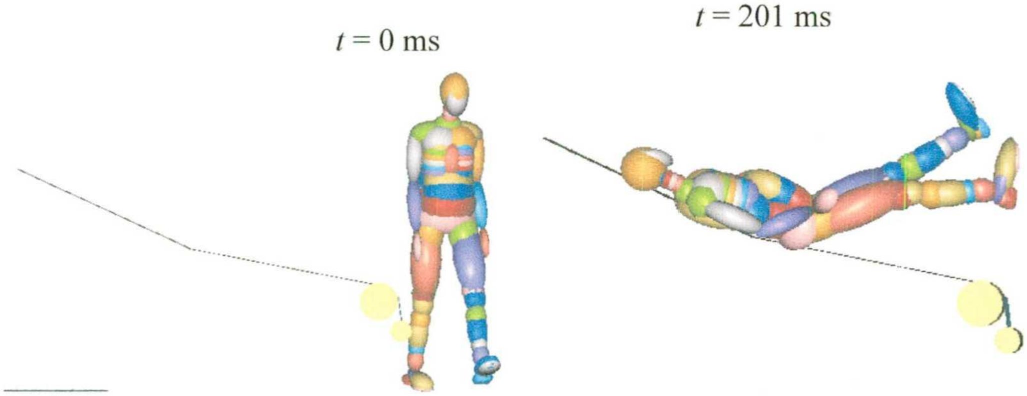

Figure 26: Screen captures from Ford Taurus simulation (initial and head contact)

Reported WAD (m)	2.30	Reported Lateral Impact Location (m)	0.30
Simulated WAD (m)	2.42	Simulated Lateral Impact Location (m)	0.32
Percent Difference	5.2%	Percent Difference	7.3%

Table 16: Comparison of the Actual and Simulated (Ford Taurus) WAD Values

Case	**Simulation**
No Reported Internal Bleeding	25% Chance ASDH on the left side of the brain (RMDM = 0.770)
No DAI Reported	15% Chance DAI (CSDM = 0.122)
No Reported Internal Contusions	15% Chance Contusion (DDM = 0.0149)
No Skull Fracture	100% Chance AIS 3 Skull Fracture (HIC = 3662)

Table 17: Ford Taurus Case injury vs. simulation results

SIMon predicted a 15% chance of a diffuse axonal injury occurring, a 15% chance of a brain contusion and a 25% chance of an acute subdural hematoma. These predicted injuries did predict accurately the injuries that were not sustained as seen in Table 17, although SIMon did correctly predict the absence of the other injuries.

3.2.7 Case #7: Honda Civic Coupe

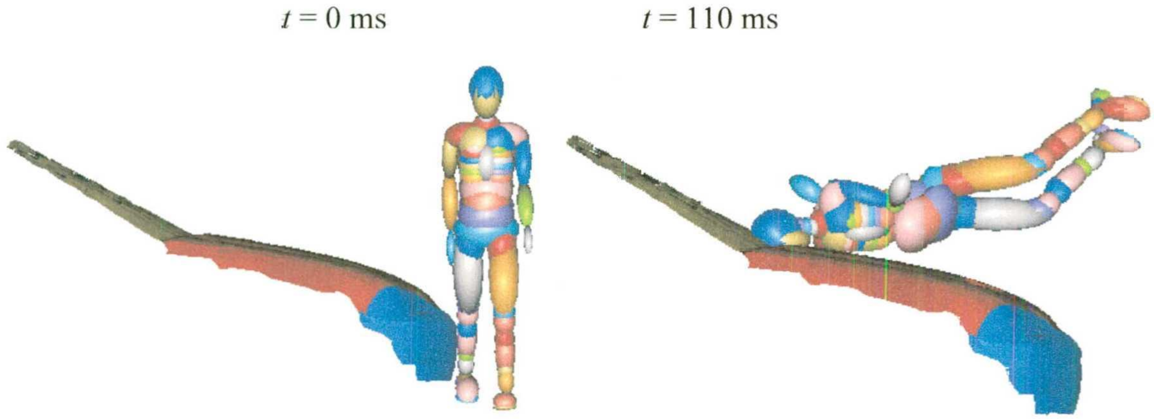

Figure 27: Screen captures from Honda Civic coupe simulation (initial and head contact)

Reported WAD (m)	1.88	Reported Lateral Impact Location (m)	0.25
Simulated WAD (m)	1.86	Simulated Lateral Impact Location (m)	0.251
Percent Difference	1.0%	Percent Difference	0.3%

Table 18: Comparison of the Actual and Simulated (Honda Civic coupe) WAD Values

Case	Simulation
Subdural Hematoma to the right side of the brain (AIS 4)	100% Chance ASDH on the right side of the brain (RMDM = 6.532)
24 hr LOC (AIS 5)	86% Chance DAI (CSDM = 0.860)
Bilateral Temporal contusions (AIS 3)	82% Chance Contusion (DDM = 0.1241)
Fracture of the Temporal Parietal Occipital bone (AIS 3)	100% Chance AIS 3 Skull Fracture (HIC = 6868)

Table 19: Honda Civic coupe Case injury vs. simulation results

SIMon predicted an 86% chance of a diffuse axonal injury occurring, an 82% chance of a brain contusion and a 100% chance of an acute subdural hematoma. Further, the HIC of this simulation correctly predicted the skull fractures seen in this case. These predicted injuries correlated well with the actual injury sustained as seen in Table 19.

3.2.8 Case #8: Chevrolet Cavalier

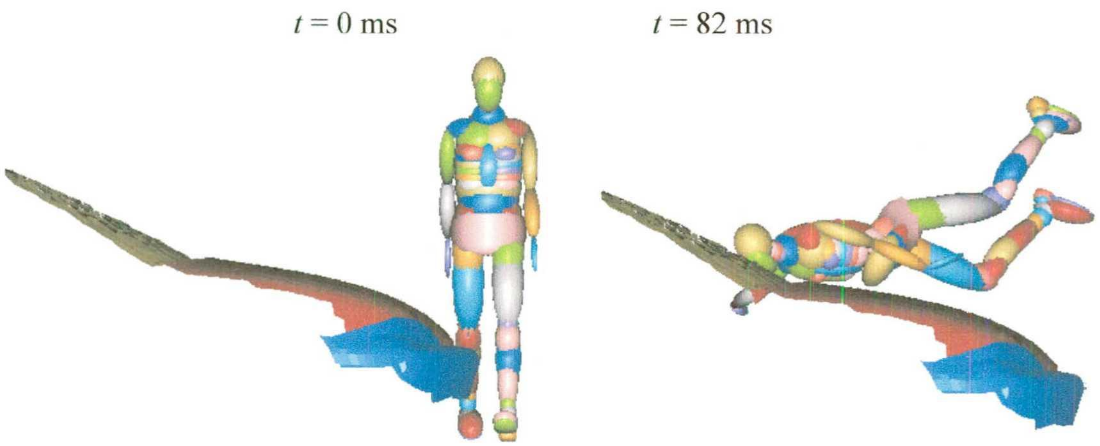

Figure 28: Screen captures from Chevrolet Cavalier simulation (initial and head contact)

Reported WAD (m)	1.90	Reported Lateral Impact Location (m)	0.37
Simulated WAD (m)	2.03	Simulated Lateral Impact Location (m)	0.38
Percent Difference	6.8%	Percent Difference	3.5%

Table 20: Comparison of the Actual and Simulated (Chevrolet Cavalier) WAD Values

Case	Simulation
Large Epidural and Subarachnoid Hematoma to Mid Brain (AIS 5)	100% Chance ASDH on the right side of the brain (RMDM = 8.172)
Coma, Unresponsive, Flaccid (AIS 5)	93% Chance DAI (CSDM = 0.925)
No Reported Contusions	100% Chance Contusion (DDM = 0.315)
Left Occipital Condyl Fracture (AIS 3)	100% Chance AIS 3 Skull Fracture (HIC = 9292)

Table 21: Chevrolet Cavalier Case injury vs. simulation results

SIMon predicted a 93% chance of a diffuse axonal injury occurring, a 100% chance of a brain contusion and a 100% chance of an acute subdural hematoma. Further, the HIC of this simulation correctly predicted the skull fractures seen in this case. These predicted injuries correlated fairly well with the actual injury sustained as seen in Table 21.

3.2.9 Case #9: Honda Civic Hatchback

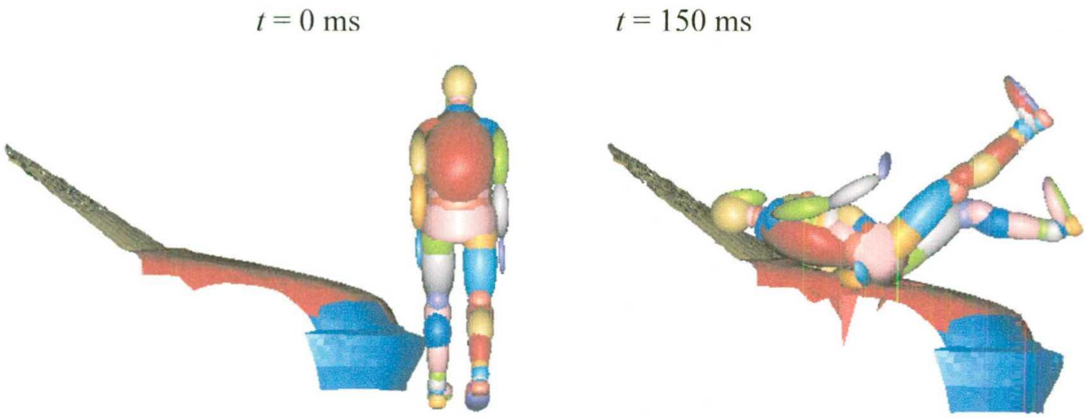

Figure 29: Screen captures from Honda Civic hatchback simulation (initial and head contact)

Reported WAD (m)	1.90	Reported Lateral Impact Location (m)	0.42
Simulated WAD (m)	1.94	Simulated Lateral Impact Location (m)	0.47
Percent Difference	2.1%	Percent Difference	12%

Table 22: Comparison of the Actual and Simulated (Honda Civic hatchback) WAD Values

Case	**Simulation**
No Bleeding Reported	86% Chance ASDH on the right side of the brain (RMDM = 1.449)
No DAI Reported	1% Chance DAI (CSDM = 0.015)
Small Right Temporal Contusions (AIS 3)	69% Chance Contusion (DDM = 0.095)
Fracture of the Temporal Parietal Lunear bone (AIS 2)	100% Chance AIS 3 Skull Fracture (HIC = 6868)

Table 23: Honda Civic hatchback Case injury vs. simulation results

SIMon predicted a 1% chance of a diffuse axonal injury occurring, a 69% chance of a brain contusion and an 86% chance of an acute subdural hematoma. Further, the HIC of this simulation correctly predicted the skull fractures seen in this case. These predicted injuries correlated fairly well with the actual injury sustained as seen in Table 23.

3.2.10 Case #10: Honda Civic Sedan

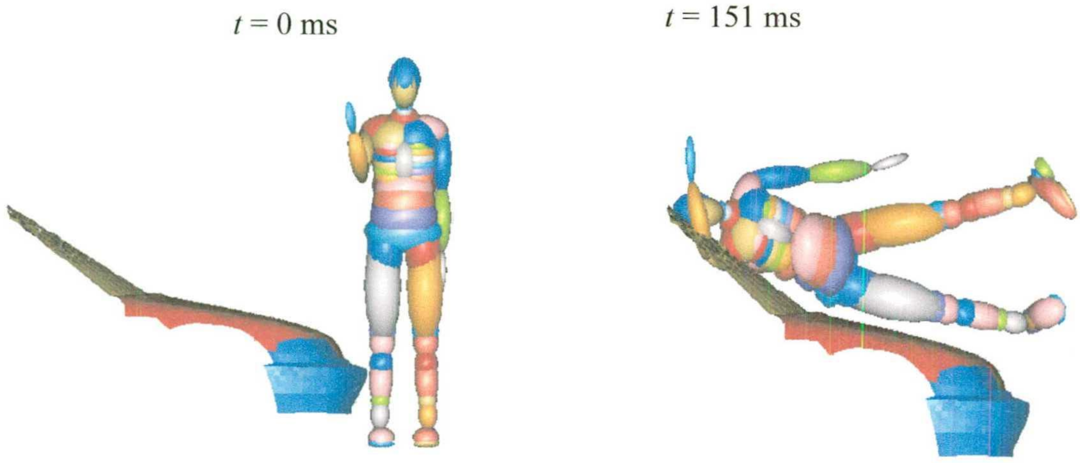

Figure 30: Screen captures from Honda Civic sedan simulation (initial and head contact)

Reported WAD (m)	2.44	Reported Lateral Impact Location (m)	0.10
Simulated WAD (m)	2.34	Simulated Lateral Impact Location (m)	0.09
Percent Difference	4.3%	Percent Difference	5.8%

Table 24: Comparison of the Actual and Simulated (Honda Civic sedan) WAD Values

Case	Simulation
No Reported Bleeding	100% Chance ASDH on the right side of the brain (RMDM = 3.160)
No Reported DAI	30% Chance DAI (CSDM = 0.14)
Bilateral Temporal contusions (AIS 3)	14% Chance Contusion (DDM = 0.041)
No Reported Fracturing	37% Chance AIS 3 Skull Fracture (HIC = 774)

Table 25: Honda Civic sedan Case injury vs. simulation results

SIMon predicted a 30% chance of a diffuse axonal injury occurring, a 14% chance of a brain contusion and a 100% chance of an acute subdural hematoma. The HIC of this simulation correctly predicted the skull fractures seen in this case. These predicted injuries did not correlate well with the actual injury sustained as seen in Table 25.

3.3 Statistical Analysis of PCDS

Figure 31 displays the data from the ten reconstruction cases performed. A linear trend line is plotted to match the data with the corresponding R^2 value given. 'Geometry' is defined as the ratio of the front-to-top transition point of the vehicle to the pedestrian height, with values ranging from 0.34 to 0.79.

Figure 32 shows the results of a logistic regression analysis of the PCDS data examining the relation between probability of injury and vehicle speed. Injury was defined as one of the four injury types that either SIMon or HIC could predict. ASDH, contusions and DAI are all lumped into one category labeled 'TBI'. The analysis was performed in SAS, as mentioned earlier. For each of these estimates, the Chi^2 value was less than 0.01%.

Figure 33 gives the probability of AIS $\geq$ 2 and AIS $\geq$ 3 head injury occurring as a function of impact velocity. Not surprisingly, the AIS $\geq$ 2 probability curve is greater than the AIS $\geq$ 3 curve because less severe injuries are more likely than more severe injuries at a given speed. These curves include injuries that SIMon and HIC predict as well as injuries that both do not predict. Again, the analysis was performed in SAS, as described earlier. For each of these estimates, the Chi^2 value was less than 0.01%.

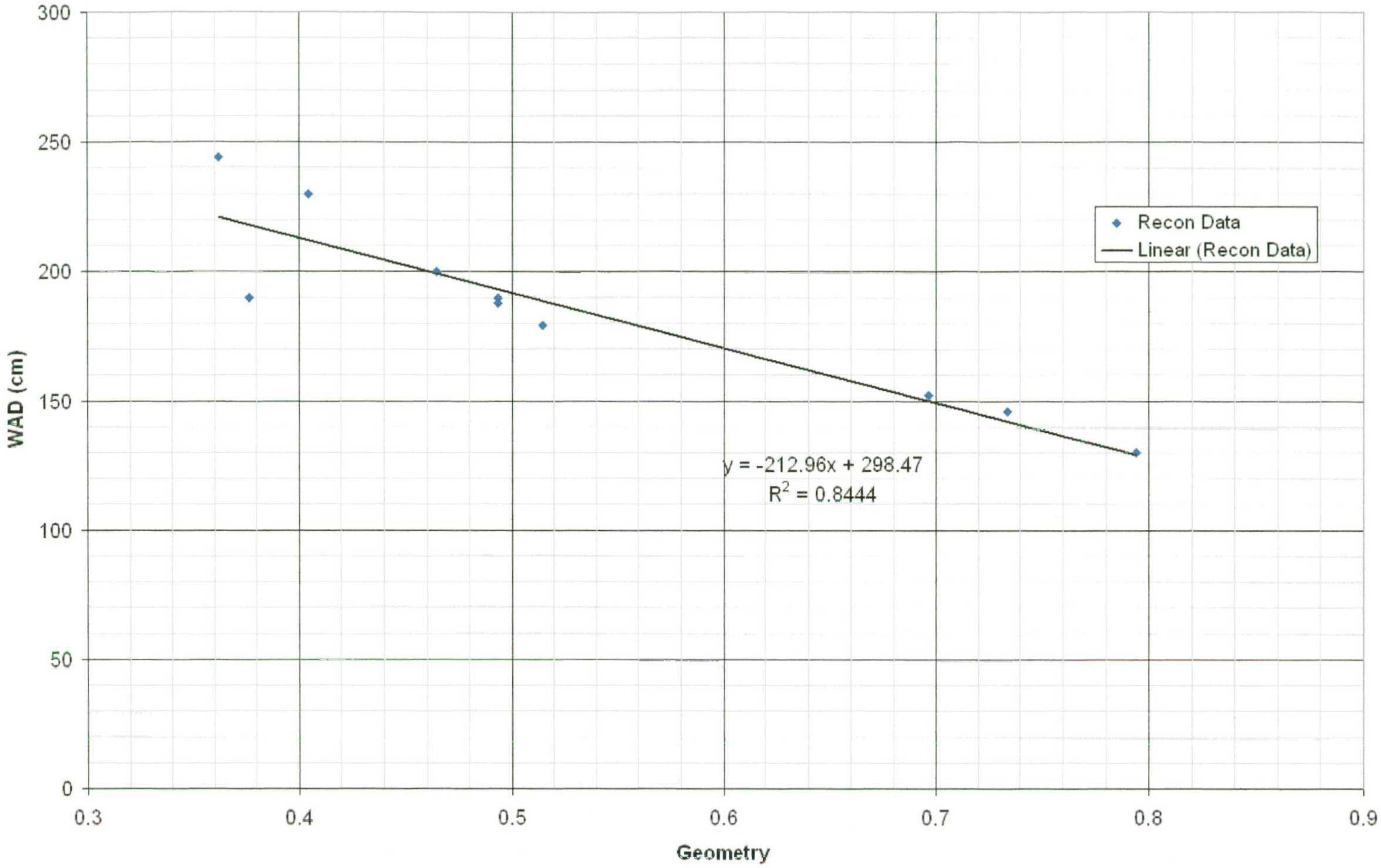

Figure 31: WAD as a function of Geometry (Front-to-Top Transition Point/Pedestrian Height) from the 10 reconstruction cases

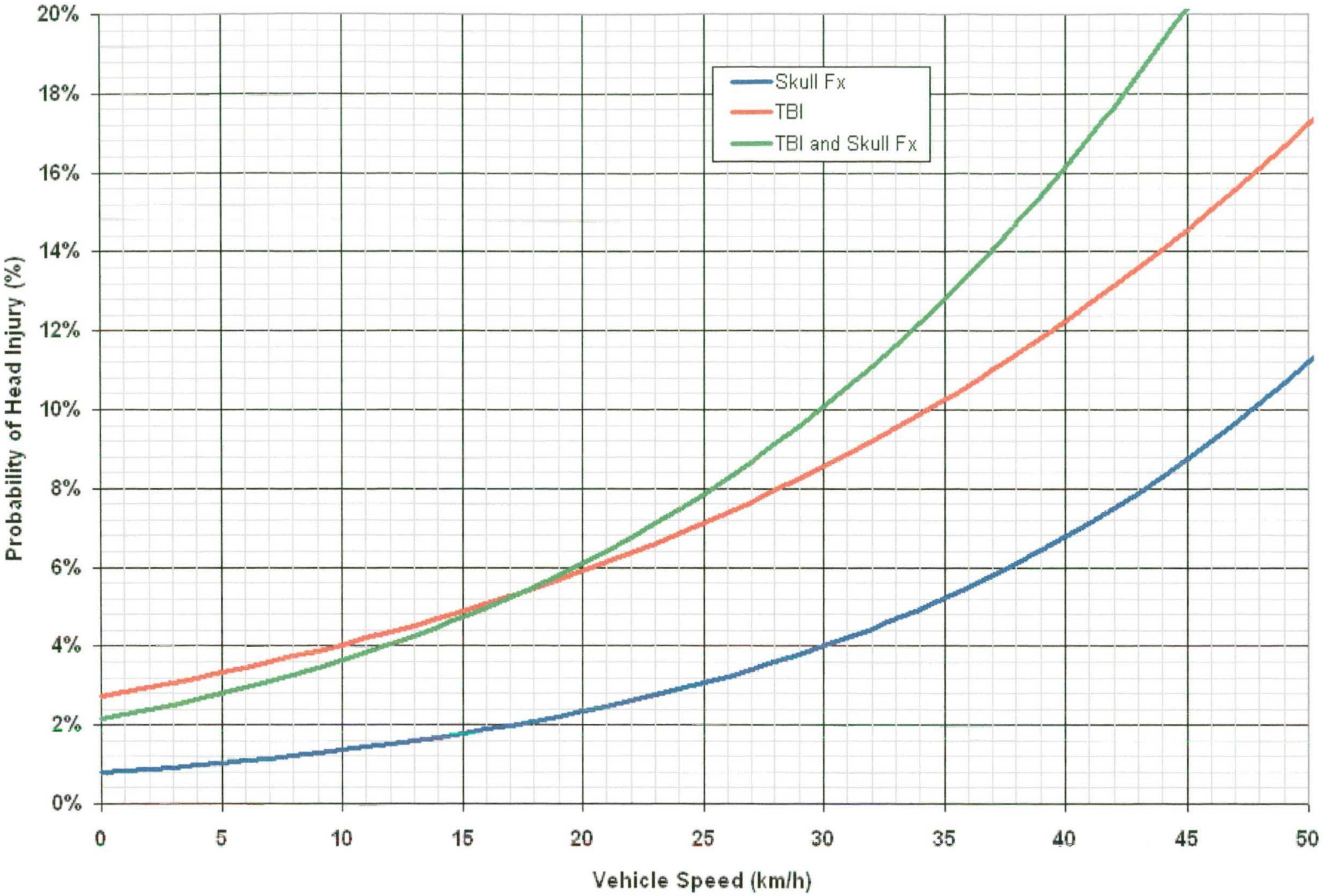

Figure 32: Probability of Injury (Injury defined as the four types of injury predicted by SIMon and HIC) as a function of Vehicle Speed (Initial impact speed)

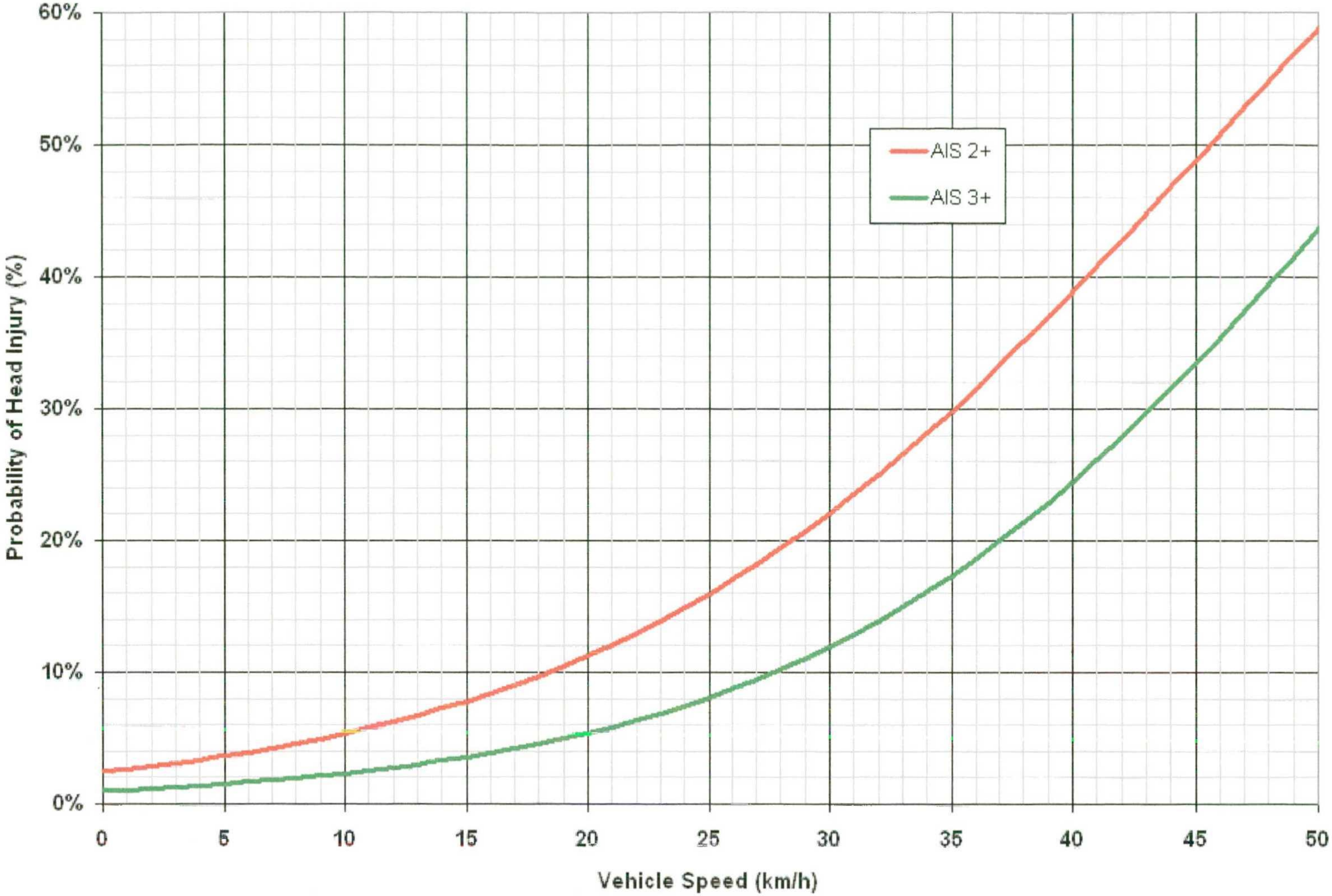

Figure 33: Probability of Injury (Injury defined as any AIS 2 and above or AIS 3 and above) as a function of Vehicle Speed (Initial impact speed)

Figure 34 gives the results of the regression analysis of the PCDS data, examining the relation between WAD as a function of both geometry and vehicle speed. The results are to a 95% confidence level. This relationship can be expressed mathematically by the formula (12):

$$WAD = 265.1 + (-190.4)x_1 + (0.6141)x_2 \tag{12}$$

WAD = Wrap around distance (cm)

x_1 = Geometry parameter (cm/cm)

x_2 = Impact Speed (km/h)

Comparison of the predicted WAD (using this formula) with the actual WAD (as reported in the ten cases examined earlier) WAD is given in Table 26. The largest percent difference being eleven percent.

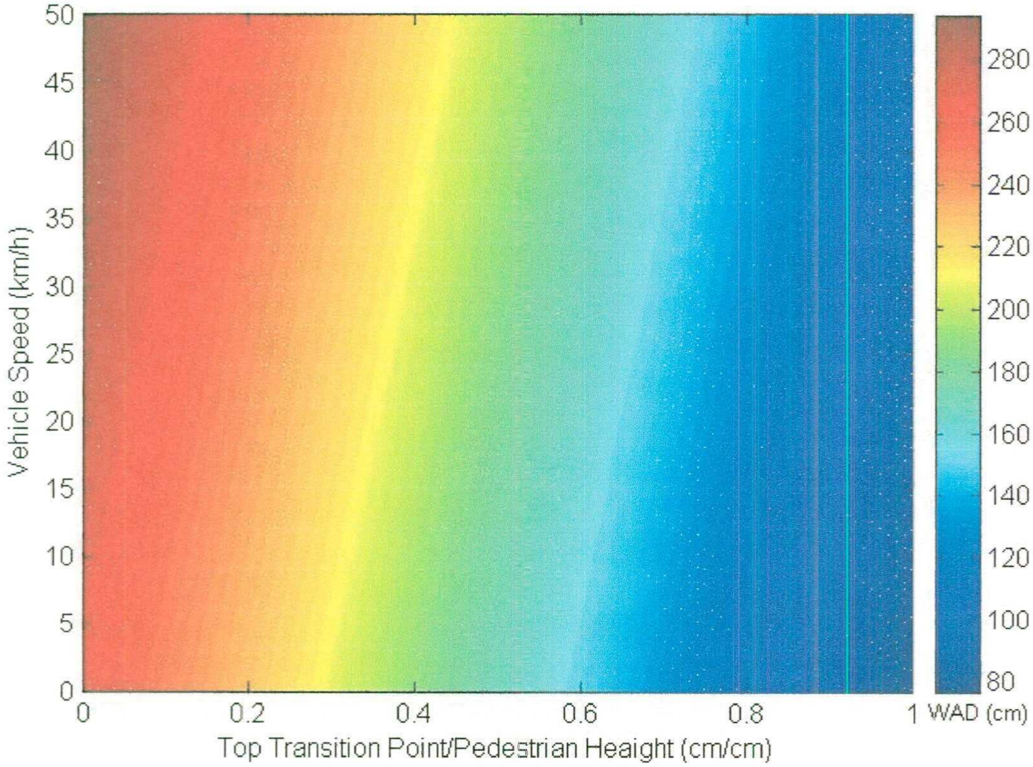

Figure 34: WAD as a function of Geometry (front-to-top transition point/pedestrian height) and Vehicle Speed

Case	WAD (Predicted)	WAD (Actual)	% Difference
Sundance	136	130	4.6%
Dodge Ram	140	146	3.9%
Celica	193	179	8.0%
Ford F150	152	152	0.1%
Voyager	194	200	3.0%
Taurus	205	230	11.0%
Civic Coupe	195	188	4.0%
Cavalier	194	190	2.2%
Civic Hatchback	191	190	0.4%
Civic Sedan	219	244	10.3%

Table 26: WAD prediction equation compared to ten reconstructions (values shown in cm)

CHAPTER 4

DISCUSSION

4.1 HIC Predictive Algorithm

The computer model of the IHRA pedestrian headform was compared to the actual headform in impact tests into both steel plates and U.S. fleet vehicles. This was done at a variety of speeds and, as a result of the different materials and locations impacted, resulted in a variety of different impact stiffness curves. Once this relationship between head impact speed, stiffness and HIC was determined, the model was then run at a variety of different linear stiffness values in order to develop a predictive HIC tool related to both impact velocity and surface stiffness. The overlaying of vehicle data on this graphical tool gave an indication of where the U.S. fleet currently falls in relation to HIC, impact velocity, and stiffness.

It was interesting that despite the significant number of experimental tests conducted, most of the HIC values were fairly small. Since the guidelines set out by the GTR did not permit testing in just one location, these low values for HIC were not attributed to testing only low stiffness locations. On one hand, it could mean that the

GTR has an excessive number of "relaxation zones", or areas of the vehicle precluded from testing, indicating a low level of stringency. On the other hand, it could indicate that current vehicles are relatively safe for pedestrians.

Calculations were done to using the potential and kinetic energy equations (6-7) to determine the maximum amount of deflection for each force-deflection curve. Even though these calculations proved accurate and were physically logical, the MADYMO model still had accuracy problems due to the approximations inherent in the IHRA headform model [8]. These problems arose from limitations in the MADYMO and are as of yet still being addressed by the software developer. In order to account for these problems and to help tune the model, a hysteresis value was given to each of the simulations. This value was based on measurements of the plastic deformation of the hood and the corresponding start of plastic deformation in the corresponding force-deflection curves derived in Matlab.

Comparison of the model to the impacts of the U.S. fleet vehicles was complicated by the nonlinear stiffness characteristics of the vehicle structures that were impacted. This nonlinear stiffness is due to a variety of factors from material composition of the hood to properties of structures underneath the hood (such as the engine block, hinges, etc.). Because of documented inaccuracies of the MADYMO model, the model was adjusted to account for this factor on a case-by-case basis using both the conservation of energy calculation and a hysteresis slope. The hysteresis would become the slope of the unloading curve for the model; an example of such is shown in Figure 35. As seen in the example and as defined in MADYMO, the hysteresis value would actually represent the slope of the unloading curve. The hysteresis unloading curve is a result of the material of the hood of the vehicle being deformed past its maximum elastic deformation, and therefore the structure cannot return to its original shape. In order to help determine the value of this hysteresis curve, the plastic deformation for each test was measured post-test. This value, together with the ending force value that resulted from the energy calculation, provided a reasonable approximation for the hysteresis slope.

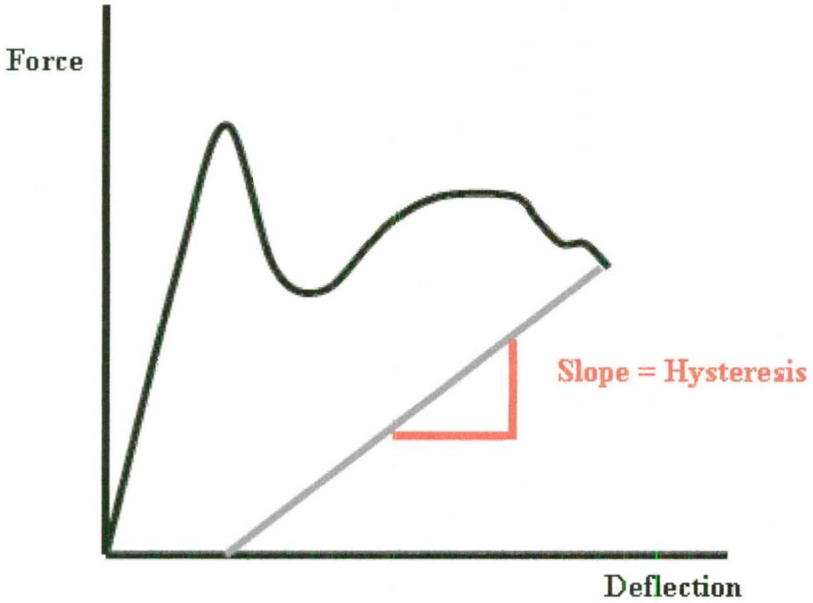

Figure 35: Example of loading, black, and unloading (hysteresis), gray, curve

Since the goal of this project was to link pedestrian crash characteristics to injury, it was required that a means of approximating a non-linear stiffness curve with a linear stiffness slope be developed so that the HIC predictive algorithm that used linear stiffness values to predict HIC could be incorporated into the final algorithm. One was to accomplish this was to relate stiffness to WAD. One method proposed was to equate the energy observed in the non-linear stiffness curve to the energy seen in a corresponding linear stiffness curve. An example of such analysis is shown in Figure 36.

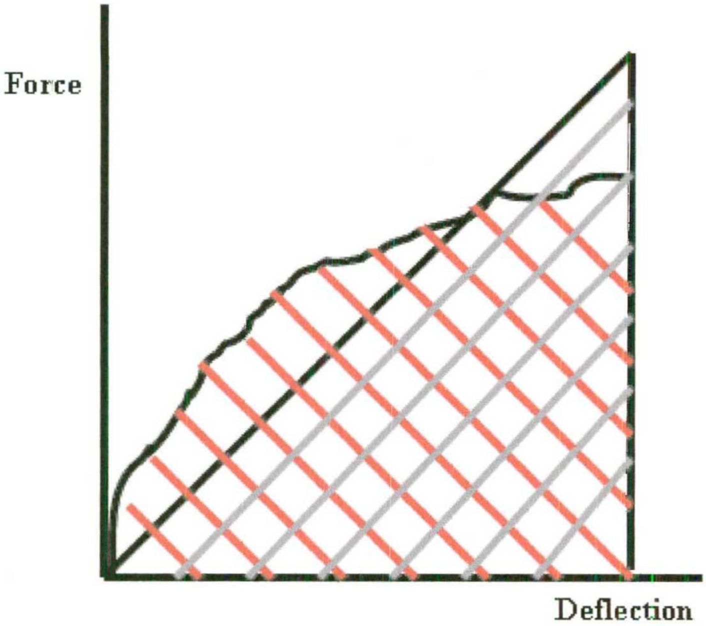

Figure 36: Conceptual example of equating the energy seen in a nonlinear stiffness curve with that seen in an equivalent linear stiffness curve that could be characterized by a single slope value. This approximation is done by equating the work done by each curve, thereby setting the red shaded area equal to the gray shaded area.

It was later determined, however, that the equating of these energies represented only a sufficient and not a necessary condition. In other words, although the energy of each stiffness curve was equal, the resulting impact characteristics were different.

A second idea for representing the nonlinear stiffness curves as a single descriptive value was devised. It was postulated that the nonlinear force-deflection curve was a superimposed combination of the force-deflection curve of the head plus the force deflection curve of the vehicle. The force-deflection properties of the headform skin could be estimated from the approximations made by Kamalakkanaan in his modeling of the IHRA headform in MADYMO [8]. This resulting force-deflection curve would then be subtracted from the total force deflection curve leaving only the vehicle force-deflection curve. An example of this approach is shown in Figure 37.

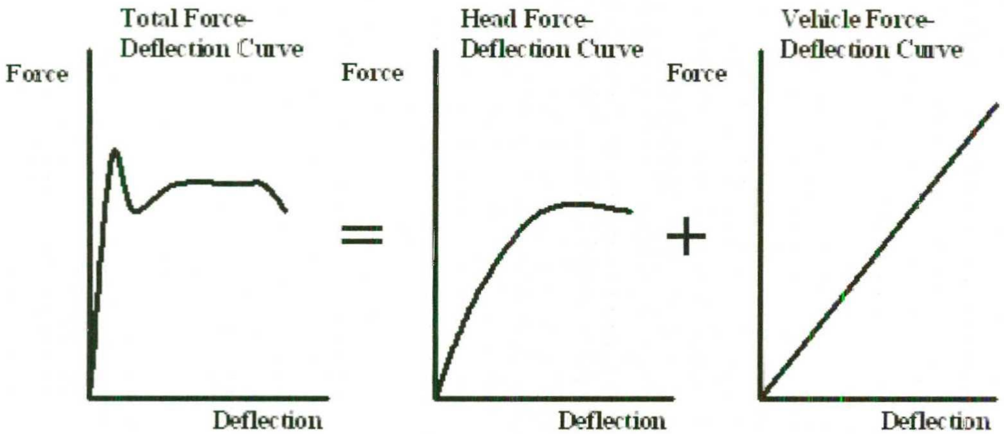

Figure 37: Conceptual example of finding the possible linear stiffness curve for a given vehicle.

This technique, however, also fell short, primarily because it was found that during impact, due to the large Poisson value of the headform skin material ($v = 0.499$), there was very minimal deflection of the skin. Therefore, the effect of the headform stiffness on the total force-deflection curve was negligible and its subtraction did not change the overall curve significantly.

Yet another option was to fit the force-deflection curve up to the first peak with a logarithmic approximation of the form $y = A\ ln(x) + B$. The coefficients would then be used to develop a relation between the value of these coefficients and the corresponding WAD of each impact. An example of this is seen in Figure 38.

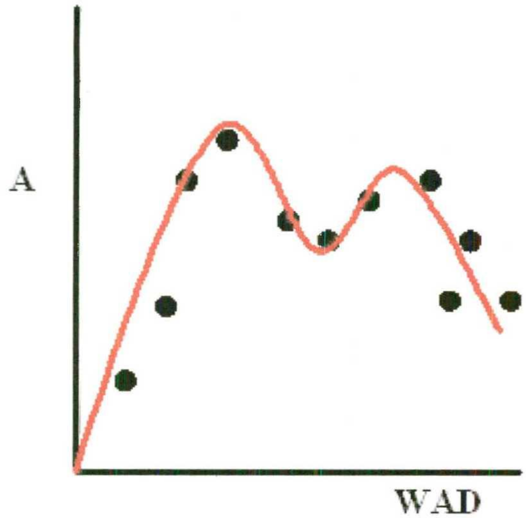

Figure 38: Conceptual example of the proposed relation between the logarithmic coefficient 'A' and WAD. The red curve represents a possible fit of the data

This was done with the assumption that the force deflection curve contained two primary portions, an elastic portion and a plastic portion, as seen in Figure 39. The elastic portion is representative of both the elastic deformation of the hood and the inertia of the hood itself. The plastic portion of the hood is representative of the membrane tension of the hood, with the hood material spreading and deforming up to a maximum deformation value at which point the headform stops from penetrating the hood any farther. Between each of these sections, there was a part of the curve that was identified as the kinetic energy absorbed by the hood collapsing.

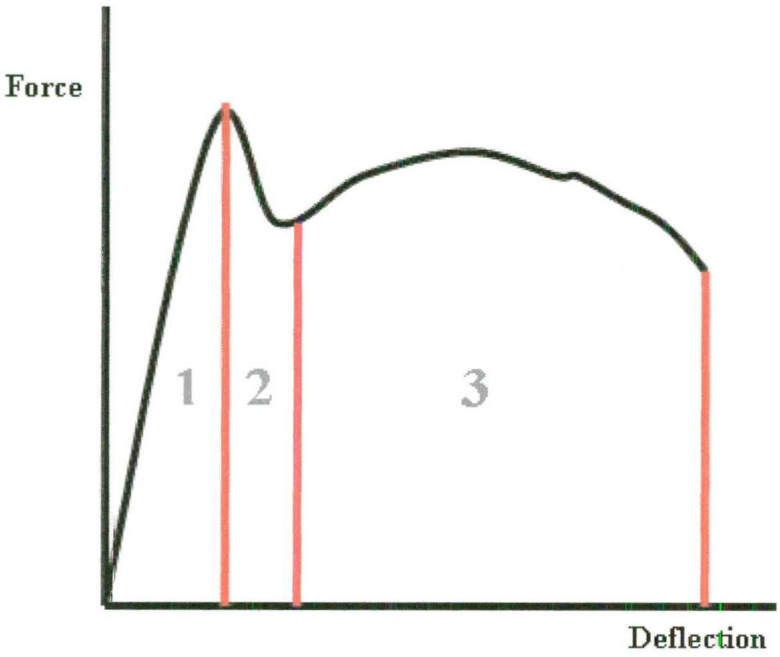

Figure 39: Example of a force-deflection curve of car impact location divided into three sections. Section 1 is the elastic deformation of the hood and the energy required to overcome the inertia of the hood. Section 2 is the energy absorbed by the hood collapsing. Section 3 represents energy absorbed by the membrane stresses in the hood, i.e. the plastic deformation.

Again, this approach was deemed insufficient for representing the stiffness of the hood structure. This was primarily due to the inability to include both coefficients '*A*' and '*B*' in a stiffness-WAD relationship as well as no apparent trends appearing for relating the coefficient '*A*' to the WAD.

Still another method was attempted that proposed to look at the slope of the force-deflection curve over small intervals and determine the maximum slope, and consequently maximum stiffness, of all of the measured stiffness slopes from each of the given intervals. This would allow the maximum slope to occur not only at the first peak, but perhaps a latter peak that occurs due to the hood coming into contact with a more rigid under-hood structure. An example of such analysis is found in Figure 40. To accomplish this method, a Matlab script was written to determine the slope over a 1 mm deflection window, move the window of data it would be sampling over by 0.01 mm, and find a new stiffness until it reached the end of the force-deflection curve. The maxima of these stiffnesses were then considered the corresponding stiffness value.

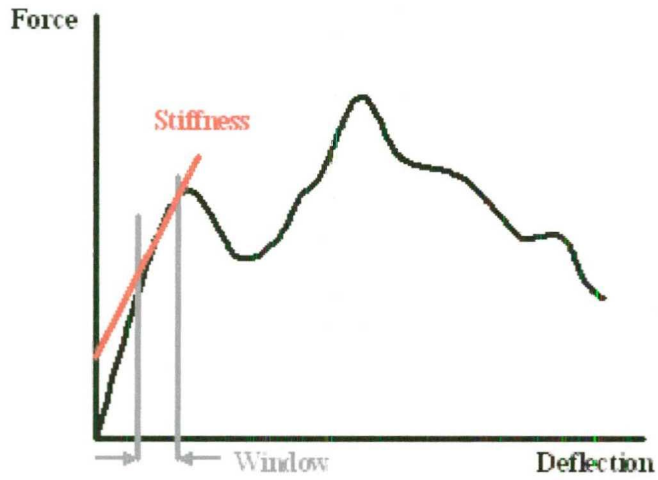

Figure 40: Conceptual example of determination of stiffness (slope of red curve) over a given window (gray) of the force-deflection curve (black)

Again, this approach did not produce the desired results. The failure of this approach was primarily due to the fact that the initial peak observed in the force-deflection curve occurred over such a small displacement that the resulting stiffness values were far too large to be considered realistic. It was also reasoned that, as in a HIC calculation, the value that was most important is not just the maximum acceleration reached but also the duration over which that acceleration persists. Similarly, it was thought that the maximum stiffness value was only a part of what contributed to injury, the second part being the distance through which a certain stiffness value persists.

From this analysis, it was hoped that clear trends would become apparent in each of the comparisons to WAD. Since each of the parameters would then vary as a function of the same variable WAD, it was hoped that these correlations could be combined and lead to a head injury prediction equation (Figure 41). However, with the problems that were encountered with the determination of a linear representation of the non-linear stiffness curves and the relation of stiffness and HIC, it was concluded that such an equation might not be possible using these parameters.

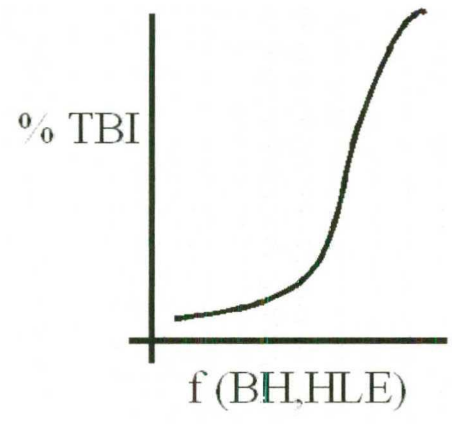

Figure 41: Conceptual example of Head Injury Prediction Equation showing how the probability of a TBI could vary as a function of physical parameters, Bumper Height and Hood Leading Edge.

The results of the drop tests, vehicle hood impact tests and the MADYMO model of impacts is shown in Figure 26 and can be used to predict HIC in a pedestrian impact given the stiffness of the hood structure and the impact velocity. This is shown graphically in Figure 43 where an impact with a specific hood gave a HIC of 2200. By altering the impact velocity and/or the stiffness, one could reduce the HIC to 1000. A reduction in head velocity would require a redesign to the geometry of the vehicle somewhere forward of the head impact location so that the majority of the pedestrian's kinetic energy is dissipated prior to head contact. A reduction in stiffness would require a redesign of the impacted structure to make it more forgiving. This graph and associated mathematical equation could provide a resource to assess the cost-benefit of such a redesign.

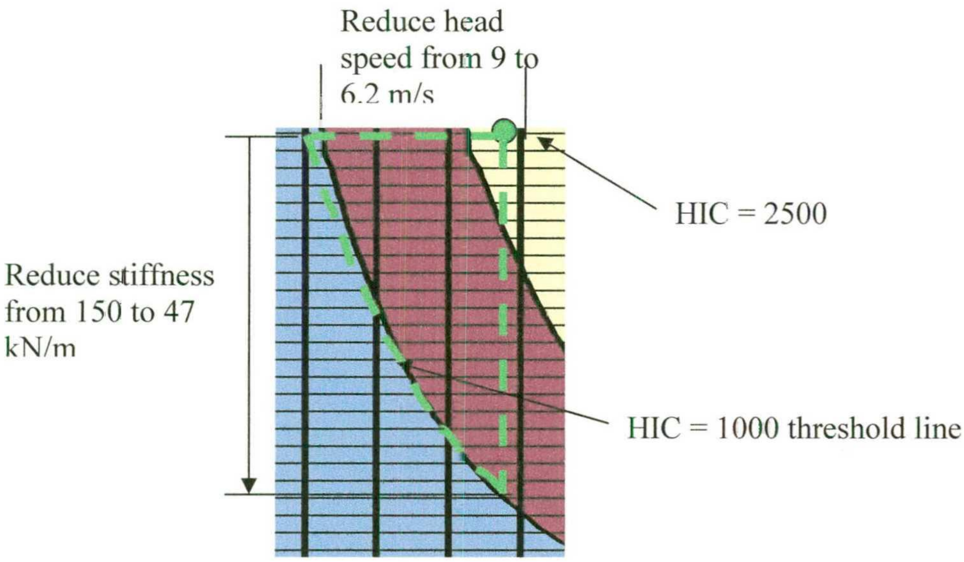

Figure 42: Design Range for Reducing HIC from 2200 to 1000

Equation showing the current design:

$$HIC = 1662 + (-8.9852)\cdot 150 + (-560.37)\cdot 9 \ldots$$
$$\ldots + (3.1904)\cdot 150 \cdot 9 + (-0.017)\cdot 150^2 + (41.157)\cdot 9^2$$
$$HIC = 2500$$

Equation showing an example of possible redesign holding stiffness constant:

$$1000 = 1662 + (-8.9852)\cdot 150 + (-560.37)x_2 \ldots$$
$$\ldots + (3.1904)\cdot 150 x_2 + (-0.017)\cdot 150^2 + (41.157)x_2^{\,2}$$
$$x_2 = 6.2 m/s$$

4.2 Case Reconstructions

The MADYMO dummy models used in this study to reconstruct PCDS cases were scaled by height and weight to match the dimensions of the victims involved in the accidents. The speed of the pedestrian perpendicular to the path of the vehicle was estimated by examining the longitudinal WAD and lateral off-center distance of first contact with the legs on the case vehicle along with the reported vehicle speed at impact. These estimated lateral speeds used to obtain the correct head impact point appeared to be reasonable as compared to the accident report. Further, minor adjustments of the impact height of the bumper and longitudinal speed were carefully made to obtain the reported head impact point. The pedestrian was reported to be running in the Sundance, Cavalier, Civic hatchback, Civic coupe and Celica cases, jogging in the Dodge Ram and Voyager cases and stopped in the Ford F150 and Civic sedan cases. Pre-impact braking was applied to slightly decrease the reported vehicle speed in the Ram, Celica, Sundance, and

F150 cases to be consistent with the case report. Table 27 summarizes the pedestrian and vehicle characteristics applied to each case.

Parameter/Case	Sundance	Ram	Celica	Voyager	F150	Taurus	Civic Coupe	Civic Hatchback	Cavalier	Civic Sedan
Dummy Model	6YO	50th Male	5th Female	50th Male	50th Male	50th Male	50th Male	5th Female	5th Female	50th Male
Height (cm)	102	165	138	183	168	178	152	150	170	196
Weight (kg)	20	57	62	83	50	82	43	57	60	98
Height/Weight (cm/kg)	5.10	2.89	2.23	2.20	3.36	2.17	3.53	2.63	2.83	2.00
WAD (cm)	130	146	179	200	152	230	188	190	190	244
WAD/Ped Height	1.27	0.88	1.30	1.09	0.90	1.29	1.24	1.27	1.12	1.24
Head Orientation at Impact (deg) (relative to vehicle)	90	0	180	0	180	90	180	0	90	90
Vehicle Speed (m/s)	10	6.7	11.8	7.8	8.9	7.5	11	8.9	18.6	10.3
Bumper Height (cm)	52	85	46	59	68	49	48	50	51	49
Hood Leading Edge (cm)	81	121	71	85	117	72	75	74	64	71

Table 27: Pedestrian and Vehicle Characteristics

Table 28 summarizes the predicted probabilities of each type of head injury and the actual injuries suffered in each case. The qualitative, point-based method of rating the accuracy of a reconstruction described by Table 3 was applied to these ten cases to illustrate the overall effectiveness of the reconstruction methodology. Four categories were created to describe this effectiveness: ‘good’, ‘fair’, ‘marginal’, and ‘poor’. A ‘good’ rating means that SIMon or HIC predicted either a (a) a high probability of injury (75 – 100%) when one did indeed occur in the case or (b) a low probability of injury (0 – 25%) when one did not occur in the case. A ‘fair’ rating means the same thing, except that the probability ranges are widened to 50 – 100% (injury) and 0 – 50% (no injury). A ‘marginal’ rating is given to an injury prediction where the probability of injury is either (a) 25-50% when one did in fact occur or (b) 50-75% when no injury of that type was present in the case. A ‘poor’ rating is given to an injury prediction where the probability of injury is either (a) under 25% when one did in fact occur (especially when it is a high AIS number) or (b) over 75% when no injury of that type was present in the case. In Table 29, these ratings are summarized for the three cases, with point values assigned to each rating that total to a relative level of effectiveness for each injury metric (good = 3, fair = 2, marginal = 1, poor = 0).

	ASDH	DAI	Contusion	Fracture	Total
Good (0 - 25%: No Injury, 75 - 100%: Injury)	6 x 3 = 18	5 x 3 = 15	5 x 3 = 15	6 x 3 = 18	22 x 3 = 66
Fair (25 - 50%: No Injury, 50 - 75%: Injury)	1 x 2 = 2	3 x 2 = 6	2 x 2 = 4	2 x 2 = 4	8 x 2 = 16
Marginal (50 - 75%: No Injury, 25 - 50%: Injury)	0	2 x 1 = 2	1 x 1 = 1	0	3 x 1 = 3
Poor (75 - 100%: No Injury, 0 - 25%: Injury)	3 x 0 = 0	0	2 x 0 = 0	2 x 0 = 0	7 x 0 = 0
Effectiveness Rating	20.0	23.0	20.0	22.0	85.0
Effectiveness Percentage	20/30 = 67%	23/30 = 77%	20/30 = 67%	22/30 = 73%	85/120 = 71%

Table 28: Effectiveness of Simulations in Reconstructing Cases

Table 28 indicates that DAI was the injury most accurately correlated to the cases, followed by brain contusions. ASDH and contusion predictions were the least effective injury measures in this series of reconstructions, although contusion prediction was slightly more effective than ASDH as it had fewer 'poor' predictions. The overall effectiveness rating was 71.0% (85 out of a possible 120 points). SIMon was 70% effective (SIMon accumulating 63 out of a possible 90 points) in predicting brain injury. HIC alone was able to accurately predict 73% of the observed skull fracture injuries.

Another means of visualizing the effectiveness of HIC in predicating head injury is found in Table 29. Here, the effectiveness of HIC to predict an AIS 3 or greater head injury is compared to both SIMon and HIC. The same point value system is used that was used in Table 29 and each of the ten reconstructed cases was evaluated. The percent risk of injury was taken to be the highest percentage given either by HIC and/or SIMon. The table shows that HIC is only 60% effective at predicting head injury while SIMon and HIC together are 63% effective.

Case #	AIS 3+ Head Injury?	HIC % Risk of AIS 3+	HIC Points	SIMon and HIC % Risk of AIS 3+	SIMon and HIC Points
1	Yes	100	3	100	3
2	Yes	4	0	99	3
3	No	99	0	99	0
4	No	29	2	99	0
5	Yes	97	3	100	3
6	No	2	3	96	0
7	Yes	100	3	100	3
8	Yes	100	3	100	3
9	Yes	5	0	45	1
10	Yes	37	1	100	3
Effectiveness Rating			18	Effectiveness Rating	19
Effectiveness Percentage			60%	Effectiveness Percentage	63%

Table 29: Effectiveness of HIC and SIMon in predicting Head injury

4.3 Statistical Analysis of the PCDS

Figure 31 pointed to a possible monotonic relationship between WAD and the defined Geometry parameter (top transition ponit/pedestrian height). This made sense since it would generally be the case that as the height of the pedestrian increased, thus decreasing the geometry parameter, the WAD would increase. However, when SAS ran the PCDS data to relate WAD as a function of geometry, no statistically significant relation was discovered. This result led to the addition of vehicle impact speed and the results seen in Figure 34. Thus, we can see that WAD is a function of the combination of both geometry and vehicle impact speed. This relationship is significant because, for a given pedestrian height, front-to-top transition point, and vehicle impact speed, a manufacturer could calculate an expected WAD. Thus a particular design could minimize the probability that a pedestrian of a particular height would strike a particularly hard surface (such as the cowl). Table 26 shows that for a representative sample of ten cases, the WAD as a function of geometry and impact velocity equation is very effective, accurately ("accurately" being defined as within a 11% difference to the actual WAD) predicting all cases.

Figures 32 and 33 show that there is a strong relationship between injury and the impact speed of the vehicle. Since SIMon only predicts the most severe brain injuries, it is no surprise that the probabilities seen in Figure 33 are higher than those in Figure 32. This is due to the fact that the SIMon predicted injuries are generally more severe, and therefore have a higher AIS rating. Figure 32 shows that in order to most effectively prevent injury one must be able to predict both TBI (or rotational injuries) and skull fracture. This can be seen by noting that the probability of a TBI occuring is higher for every impact velocity. Figure 33 shows that as the sample size is increased and all the possible head injuries that may occur are examined (AIS ≥ 2 or AIS ≥ 3), the probability of sustaining a head injury significantly increases.

In order to determine the effectiveness of the GTR on mitigating all head injuries, the 2003 Dodge Ram GTR test and the 1996 Dodge Ram case reconstruction were examined. The pedestrian involved in the accident would be placed into the 50th percentile male ("adult") category as directed by the GTR testing procedures. However, the reported WAD of 146 cm (Table 8) is well below the adult cut-off line of 170 cm. This being the case, the child headform impact location was used since it most closely matched the case WAD and lateral location. From the simulations, the HPA model gave a

HIC of 1204 (71.6% chance of an AIS $\geq$ 3 skull fracture). Through the reconstruction process with SIMon, SIMon predicted a 33% chance of a diffuse axonal injury occurring, a 48% chance of a brain contusion and a 99% chance of an acute subdural hematoma (Table 9). Finally, the WAD prediction equation (12) gave the WAD to within a 3.9% error (Table 26). Comparing these predicted injuries to the actual injuries, it is observed that the reconstruction process is more effective than using HIC alone, accurately predicting the most severe injury as well as the absence of a skull fracture (Table 9). This example also illustrates the limitations in the WAD definitions as given by the GTR since the WAD for this case was far outside of the Adult zone. The example also shows the usefulness of the WAD prediction equation in determining potential WAD locations for given pedestrian heights.

CHAPTER 5

CONCLUSIONS

Tables 4 and 5 showed that the IHRA headform model is valid for a range of head impact speeds between 3.5 and 8.06 m/s as indicated by the consistency of experimental and simulated HIC values. All of the percent differences between the experimental and simulated HIC values were below 10%, with the majority of differences being very low. Overall, the experimental HIC values were low with about 25% exceeding 1000 and the largest HIC reaching nearly 2200. The performance of the model for these less aggressive impacts as well as the small amount of higher HIC impacts implies that it would still do quite well for simulating more aggressive impacts. Also, during the course of the experimental testing, it was noted that vehicle manufacturers have started to implement energy absorbing structures into the design of their hoods, indicating that very high HIC values are becoming less prevalent.

With the model validated for a range of impact velocities and stiffness values, Figure 20 provides a useful guide for modifying the stiffness and/or geometry of a specific vehicle location to meet a HIC performance requirement. It is interesting to note that the model performed better using the linear stiffness than when the non-linear stiffness was applied. Further, modifications were required of the headform model when non-linear stiffness curves were applied. These included hysteresis values being added to the model to simulate the unloading of the hood structure. In all, the computer model provides a useful way to measure the aggressiveness of a particular structure.

The expansion of the database (Figure 20) from those values gained through testing (red and yellow points on Figure 20) to encompass a broad range of stiffness values and impact velocities demonstrates one of the principle advantages of such modeling. A validated model may prove useful in reducing both time and cost in the development and evaluation of a system. However, the limits of the code itself and the approximations made indicate that the model still leaves room for improvement. Primarily, improvements to how the force-deflection curve, and consequently the stiffness, is modeled and implemented into MADYMO will have the effect of both improving the results and making the simulation of vehicle impacts more repeatable. Although this is the case, the model is still able to help make valid inferences of the effects of both head impact speed and stiffness on HIC, as well as the relationship of these three parameters.

The ten reconstruction cases showed that SIMon is a useful tool in determining the effect of vehicle structure geometries on pedestrian brain injury risk. From Tables 28 and 29, we can see that SIMon is very effective at predicting brain injury, and thus is a good tool for both evaluation and design. Further, when combined with HIC, the majority of potential injuries were accurately predicted. Therefore, it is necessary to use both a linear and rotational injury predictor to adequately predict injury and mitigate a larger portion of injurious scenarios for pedestrians.

This necessity is illustrated in Table 28, and from the given example of HIC's effectiveness at predicting the presence or absence of any head injury, it is clear that HIC is insufficient for predicting all pedestrian head injuries because it was only 60% effective in this study. This is also illustrated in Figure 34 where it is shown that skull fracture has a lower probability of occurring than a TBI does for a given vehicle impact speed.

Figure 34 (the relationship between WAD, geometry and impact speed) provides a useful tool for the design of vehicles to help isolate dangerous structures from head impact. In Figure 20, it is clear that more rigid structures would be more aggressive in impact situations. Therefore, vehicle designers could research the average vehicle impact velocities as well as the most common pedestrian heights in those accidents involving their vehicle models. With this information, the designers could then adjust the front of the vehicle in order to manipulate the front-to-top transition point of the vehicle to place the particular pedestrian at a certain WAD where severe head injury risk could be minimized.

This study has produced three tools for the evaluation of vehicles in pedestrian accidents. The first tool is the HIC predictive algorithm (HPA) that provides a means for minimizing the HIC value for a given head impact velocity and impact stiffness. The second tool is SIMon and its use in conjunction with full body reconstructions. This reconstruction methodology can be used to analyze how the front-end geometry of a vehicle produces certain types of TBI. The third tool comes from the results of the statistical analysis on the PCDS. Since it had been shown in the HIC predictive algorithm that more rigid structures would cause more injuries and that head impact velocity would have an effect on the probability of injury, the relationship developed between WAD, the geometry parameter (front-to-top transition point divided by pedestrian height) and vehicle impact velocity provides another useful tool for design of vehicles in order to minimize the chances of a pedestrian striking a particularly rigid surface such as the cowl. Figure 43, 44, 45 summarizes the three tools developed in this study.

An example of how these tools could be applied is as follows. Given field data shows that most of the pedestrians struck are a certain height and are hit at a certain speed. The WAD predictive equation (Tool #3) gives the approximate head impact location for these pedestrians. Next, using the reconstruction process (Tool #2) the probability of injury is calculated using SIMon and HIC. Finally, the HIC predictive algorithm (Tool #1) is employed to calculate the redesign required (if necessary) in head impact speed and/or stiffness which would correspond to changes of geometry and/or material characteristics. Each of these tools could also be used independently to evaluate the aggressiveness of a vehicle. The HIC predictive algorithm could give the HIC values for a range of impact points given the corresponding stiffness and head impact velocity. The reconstruction process could be used to analyze the kinematics of pedestrians during vehicle impacts. Finally the WAD predictive equation could determine the required geometry changes to place the head impact point in relatively soft areas of the front profile such as the windshield.

$$HIC = 1662 + (-8.9852)x_1 + (-560.37)x_2 \mathrm{K}$$

$$\mathrm{K} + (3.1904)x_1 x_2 + (-0.017)x_1^{\ 2} + (41.157)x_2^{\ 2}$$

HIC = Head Injury Criteria

x_1 = Linear Stiffness (kN/m)

x_2 = Impact Speed (m/s)

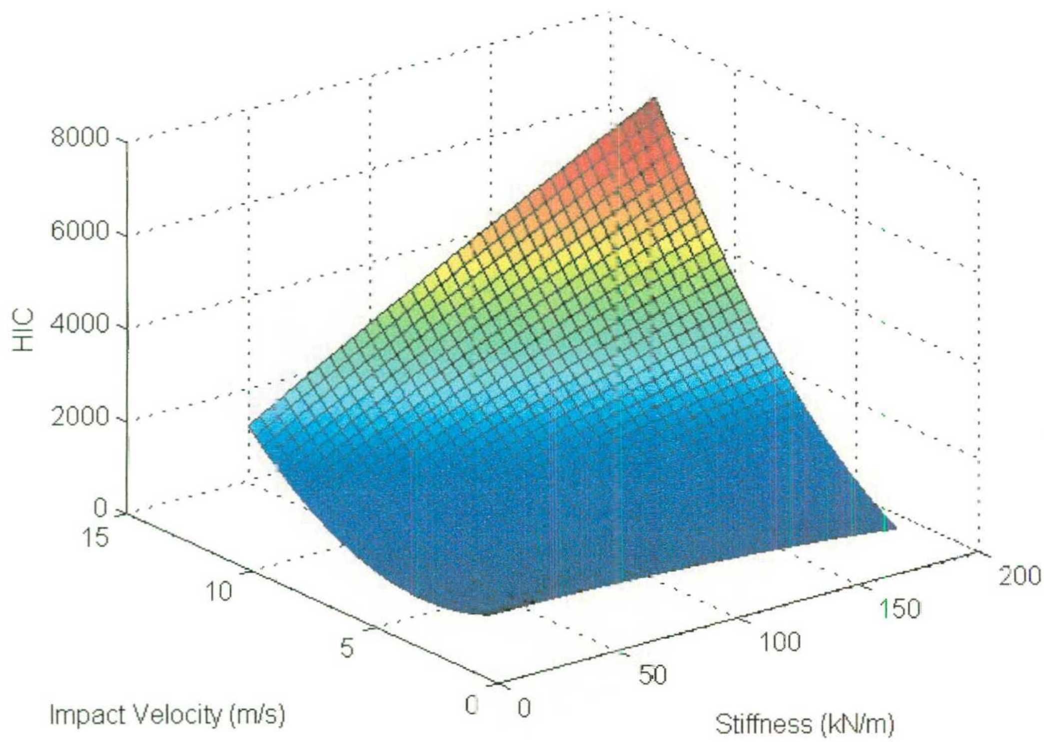

Figure 43: Three tools developed in this study; Tool #1: HIC Predictive Algorithm

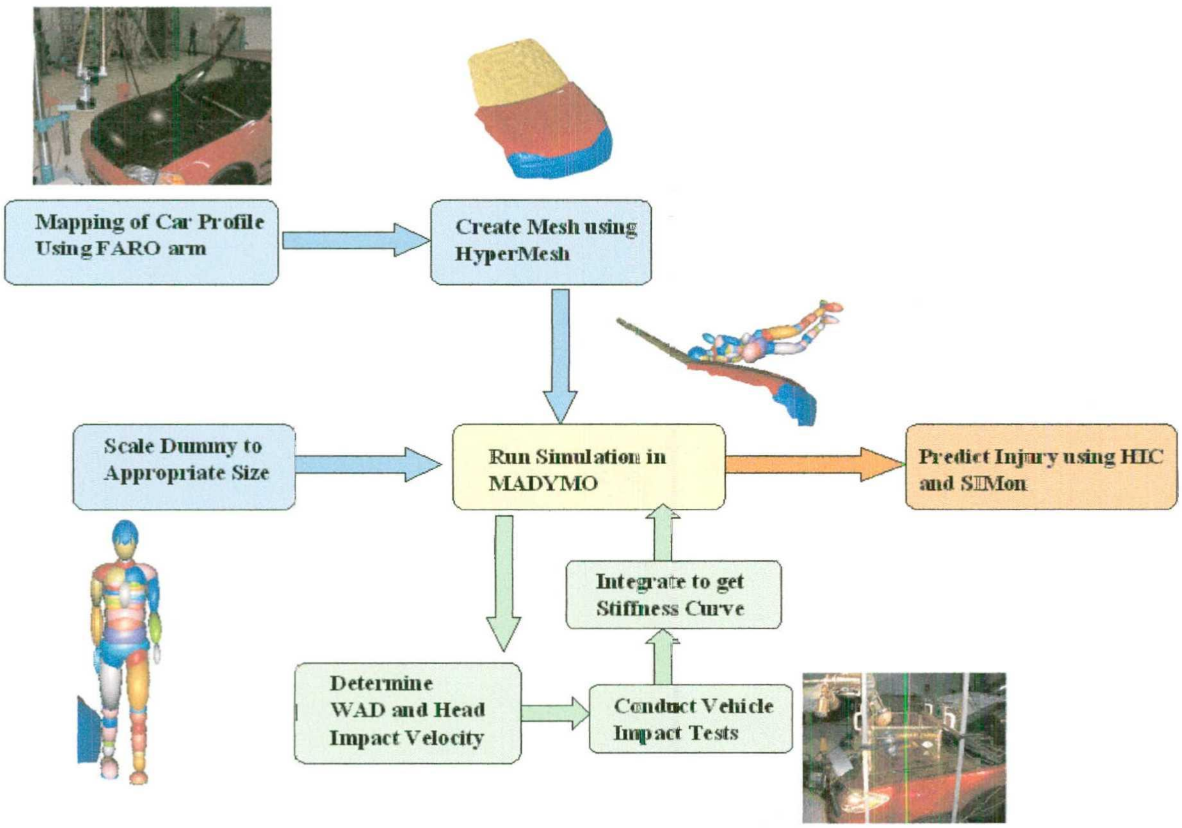

Figure 44: Three tools developed in this study; Tool #2: Reconstruction Process

$$WAD = 265.1 + (-190.4)x_1 + (0.6141)x_2$$

WAD = Wrap around distance (cm)

x_1 = Geometry parameter (cm/cm)

x_2 = Impact Speed (km/h)

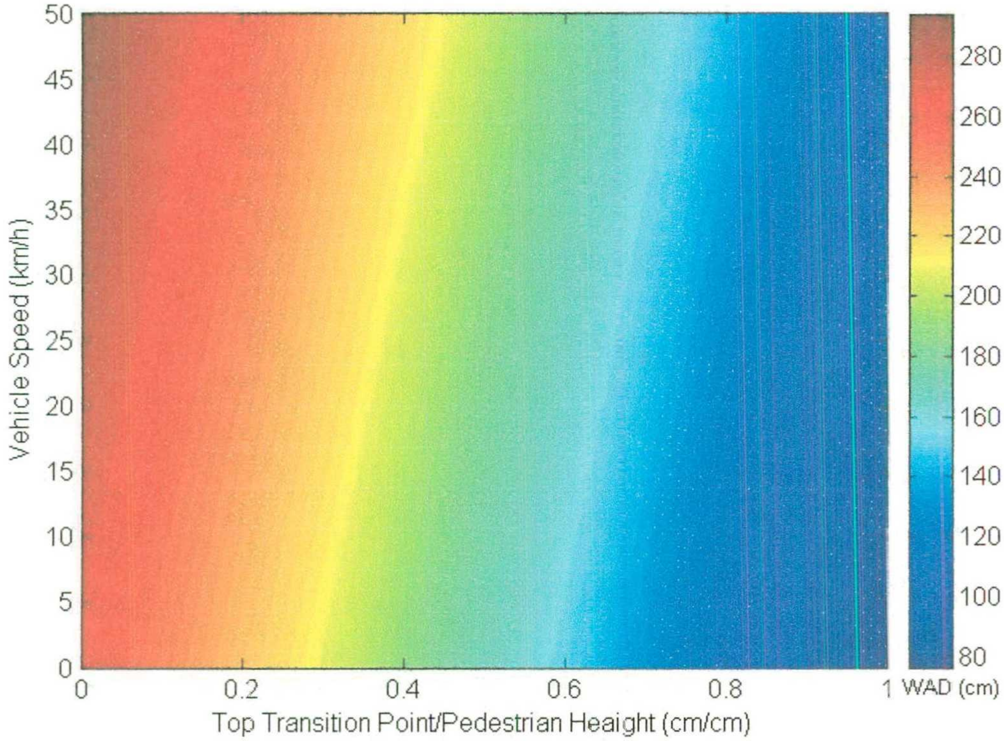

Figure 45: Three tools developed in this study; Tool #3: WAD Predictive Algorithm

CHAPTER 6

RECOMMENDATIONS

In the future, there are several areas related to this study that should be explored. First, the IHRA headform computer model that was used in this study still has limitations in its measuring the response of a non-linear stiffness. Finding which characteristics of a non-linear stiffness curve would have the most effect on HIC or the different types of brain injury would be a very large step in improving head injury prediction, considering most vehicle structures have non-linear stiffness characteristics (see Figure 17). Further work that could be done on the IHRA headform model would be examine if the model is valid for rotation and how this would affect injury prediction.

Another area to be further explored would be the relationship between head injury and the various accident parameters (pedestrian characteristics, vehicle characteristics, impact speed, etc.). Even though no monotonic relationship was found to exist, it is still believed that such a relation is possible. This would help complete the connection between the controllable characteristics of a vehicle or crash and the subsequent injuries.

REFERENCES

1. Abel, J. Gennarelli, T.A., Seagawa, H. "Incidence and severity of cerebral concussion in the rhesus monkey following sagittal plane angular acceleration." Proc. 22nd Stapp Car Crash Conference, pp. 33-53, 1978. Society of Automotive Engineers, Warrendale PA.

2. Allsop, D.L., Warner, C.Y., Wille, M.G., Schdider, D.C., Nahum, A.M. "Facial impact response-A comparison of the Hybrid III dummy and human cadaver." Proc. 32nd Stapp Car Crash Conference, SAE Paper No. 881719, 1988. Society of Automotive Engineers, Warrendale, PA.

3. Brooks, D.L., Wiechel, J.F., Sens, M., Guenther, D.A., "Review of Pedestrian Impact Reconstruction," Accident Reconstruction: Automobiles, Tractor-Semi Trailers, Motorcycles, and Pedestrians, Publication No. P-193, Society of Automotive Engineers, 1987.

4. Chidester, A.C.D., Isenberg, R. A. June, 2001. "Final Report – The Pedestrian Crash Data Study." Proceedings of the 17th International Technical Conference on the Enhanced Safety of Vehicles (ESV) Conference, June 4-7, 2001 in Amsterdam, The Netherlands. National Highway Traffic Safety Administration, Washington, DC. DOT HS 809 220, June 2001. Paper Number 248, 12 pgs.

5. Hardy, W.N., Foster, C.D., Mason, M.J., Yang, K.H., King, A.I., Tashman, S. "Investigation of Head Injury Mechanisms Using Neutral Density Technology and High-Speed Biplanar X-Ray." Stapp Car Crash Journal, Vol. 45 (November 2001), pp. 337-368

6. "International Harmonized Research Activities Pedestrian Safety Working Group 2001 Report", IHRA/PA/200.

7. Kallieris, D., Rizzetti, A., Mattern, R. "Some Observations to the Skull-Brain

Trauma." Proc. AGARD Conference 597, pp. 1-4. (1997) Advisory Group for Aerospace Research and Development, Neuilly-Sur-Seine, FR.

8. Kamalakkannaan, S.B. "Modeling of the IHRA Pedestrian Head-form Impactor." Master's Thesis, The Ohio State University 2004.

9. Meaney, D.F., Smith, D., Ross, D.T., Gennarelli, T.A. "Diffuse axonal injury in the miniature pig: Biomechanical development and injury threshold." ASME Crashworthiness and occupant protection systems, 1993. 25: 169-175.

10. Mizuno, Y. "Summary of IHRA Pedestrian Safety WG Activities (2003) – Proposed Test Methods to Evaluate Pedestrian Protection Afforded by Passenger Cars." Japan Automobile Standards Internationalization Center (JASIC), Chairman on behalf of IHRA / P.S. WG, 580, 2003.

11. Nahum, A.M., Smith, R., Ward, C.C. "Intracranial pressure dynamics during head impact." Proc. 21st Stapp Car Crah Conference, SAE Paper No. 770922, 1977. Society of Automotive Engineers, Warrendale, PA.

12. Nusholtz, G.S., Wylie, B. Glascoe, L.G. "Cavitation/boundary effects in a simple head impact model." Aviation Space & Enviromental Medicine, 1995. 66(7): 661-667.

13. Nyquist, G.W., Cavanaugh, J.M., Goldber, S.J., King, A.I. "Facial impact tolerance and response." Proc. 30th Stapp Car Crash conference, SAE Paper No. 861896, 1986. Society of Automotive Engineers, Warrendale, PA.

14. Stalnaker, R.L., Alem, N.M., Benson, J.B., Melvin, J.W. "Validation studies for head impact injury model." Final report DOT HS-802 566, 1977. National Highway Traffic Safety Administration, U.S., Department of Transportation, Washington, DC.

15. Sens, M.J., Wiechel, J.F., Cheng, P.H., Marandi, M., Guenther, D.A. "The Vocabulary of Accident Reconstruction," Society of Automotive Engineers, Warrendale, Pennsylvania, 1989.

16. Sens, M.J., Cheng, P.H., Wiechel, J.F., Guenther, D.A. "Perception/Reaction Time Values for Accident Reconstruction," Paper No. 890732, Society of Automotive Engineers, Warrendale, Pennsylvania, 1989.

17. Takhounts, E.G., Eppinger, R.H., Campbell, J.Q., Tannous, R.E., Power, E.D., Shook, L.S., "On the Development of the SIMon Finite Element Head Model." Stapp Car Crash Journal, Vol. 47 (October 2003), pp. 107-133

18. Trosseille, X., Tarriere, C. Lavaste, F., Guillon, F., Domont, A. "Development of a F.E.M. of the human head according to a specific test protocol." Proc. 36th Stapp Car Crash Conference, SAE Paper No. 922527, 1992. Society of Automotive Engineers, Warrendale, PA.

19. TNO (2003): "MADYMO Theory Manual, Version 6.1," TNO-Automotive, Delft, The Netherlands.

20. Vorst, M.V., Stuhmiller, J., Ho, K., Yoganandan, N., Pintar, F., "Statistically and Biomechanically Based Criterion for Impact-Induced Skull Fracture." 2001.

21. Wiechel, J.F., Guenther, D.A., Roberts, V.L., "An Interactive Computer Graphics Simulation of a Vehicular Crash," Proceedings, Canadian Multidisciplinary Road Safety Conference III, May 27-30, 1984, London, Ontario.

22. Wiechel, J.F., Brooks, D.L., Stansifer, R.L., Guenther, D.A., "Pedestrian Accident Investigation and Reconstruction," Proceedings, Canadian Multi-disciplinary Road Safety Conference V, June 1-3, 1987, Calgary, Alberta.

23. Wiechel, J.F., MacLaughlin, T.F., Guenther, D.A., "Head Impact Reconstruction – HIC Validation and Pedestrian Injury Risk," Paper No. 930895, Society of Automotive Engineers, Detroit, Michigan, 1993.

24. Working Party on Passive Safety (GRSP). "Proposal for a Global Technical Regulation on Uniform Provisions Concerning the Approval of Vehicles With Regard to Their Construction in Order to Improve the Protection and Mitigate the Severity of Injuries to Pedestrians and Other Vulnerable Road Users in the Event of a Collision."

Economic Commission for Europe, World Forum for Harmonization of Vehicle Regulations (WP.29) 7 March 2005.

25. Zhang, L., Yang, K.H., Dwarampudi, R., Omori, K., Li, T., Chang, K., Hardy, W., Kahlil, T.B., King, A.I. "Recent Advances in Brain Injury Research: A New Human Head Model Development and Validation." Stapp Car Crash Journal, Vol. 45 (November 2001), pp. 369-394.